Chapter 2
Distributed Detection of Spatially Constant Phenomena

In this chapter, we analyze the problem of distributed detection of a spatially constant phenomenon in IEEE 802.15.4-based Wireless Sensor Networks (WSNs). We first present a communication-theoretic framework on distributed detection in clustered sensor networks with tree-based topologies and hierarchical multi-level fusion. The sensor nodes observe a binary phenomenon and transmit their own data to an Access Point (AP), possibly through intermediate Fusion Centers (FCs), which perform majority-like fusion strategies. Note that the AP functionality is concentrated in the Personal Area Network (PAN) coordinator and this notation is used to highlight the fact that the AP is the network collector. Moreover, the FCs correspond, according to an IEEE 802.15.4 notation, to Full Function Devices (FFDs), whereas the sensors are implemented through Reduced Function Devices (RFDs). We investigate the impact of uniform and non-uniform clustering on the system performance, evaluated in terms of probability of decision error on the phenomenon status at the AP. Our results show that, in the absence of inter-node interference (low traffic load), uniform clustering leads to minimum performance degradation, which depends only on the number of decision levels, rather than on the specific clustered topology.

Since the uniform clustering topology allows to reduce the performance loss incurred by multi-level information fusion, we then investigate the benefits, in terms of longer network lifetime, of *adaptive reclustering*. In particular, lifetime is studied under a physical layer Quality of Service QoS constraint, given by the maximum tolerable probability of decision error at the AP. On the other hand, *absence of reclustering* leads to a shorter network lifetime, and we show the impact of various clustering configurations under different QoS conditions. Our results show that, in the absence of inter-node interference, the organization of sensors in a *few big clusters* is the winning strategy to maximize network lifetime. Moreover, the observation of the phenomenon should be *frequent* in order to limit the penalties associated with the reclustering procedure.

C. Buratti et al., *Sensor Networks with IEEE 802.15.4 Systems*,
Signals and Communication Technology, DOI: 10.1007/978-3-642-17490-2_2,

Although our analysis is based on the assumption of constant Signal-to-Noise Ratio (SNR) at the sensors, we show how to extend it to sensor networks characterized by *non-constant* observation SNRs at the sensors. Furthermore, we show *how* the impact of communication noise in the links between the sensors and the AP depends on the sensor SNR profile (i.e., the spatial distribution of the observation noise). More precisely, different sensor SNR profiles are compared under two alternative assumptions: (i) common *maximum* sensor SNR or (ii) common *average* sensor SNR. Finally, we study how to combine decoding and fusion at the AP to improve the performance in scenarios where the sensors communicate to the AP through *noisy* communication links. Simple distributed channel coding strategies are considered, using either repetition coding at each sensor (i.e., multiple observations) or distributed (network-wide) systematic block channel coding. In the latter case, the use of a relay is proposed. In all cases, the system performance is analyzed *separating* or *joining* the decoding and fusion operations at the AP. Our results show that the schemes with joint decoding and fusion show a significant performance improvement with respect to that of schemes with separate decoding and fusion and the use of *multiple observations* is often the winning choice at practical values of the probability of decision error.

The analytical approach introduced in this chapter is extended to realistic sensor networks, based on commercial protocols. In particular, simulation and experimental (relative to IEEE 802.15.4-based networks) results, which confirm the analytical predictions, are presented, enriching the proposed analytical framework and showing how typical networking performance metrics (such as throughput and delay) are influenced by the probability of decision error.

This chapter is structured as follows. In Sect. 2.1, we present the analytical framework to analyze the performance of distributed detection schemes in clustered sensor networks. In Sect. 2.2, we analyze the sensor network lifetime in the presence of the proposed distributed detection strategies. In Sect. 2.3, we extend our framework to take into account possible non-constant SNR spatial distributions at the sensors. In Sect. 2.4, we extend the framework also to take into account the presence of different detection/fusion strategies. In Sect. 2.5, concluding remarks are given and, finally, a brief review of the literature is presented in Sect. 2.6.

2.1 Distributed Detection in Clustered Sensor Networks

2.1.1 Preliminaries on Distributed Binary Detection

We consider a network scenario where n sensors observe a *common binary phenomenon* whose status is defined as follows:

$$H = \begin{cases} H_0 & \text{with probability } p_0 \\ H_1 & \text{with probability } 1 - p_0 \end{cases}$$

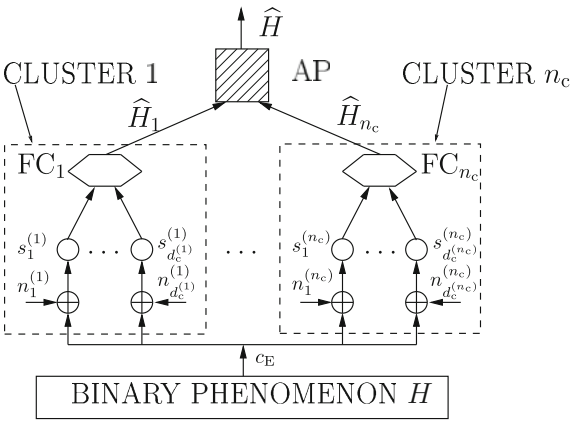

Fig. 2.1 Block diagram of a clustered sensor network with distributed binary detection and two decision levels

where $p_0 \triangleq \mathbb{P}\{H = H_0\}$, being $\mathbb{P}\{\cdot\}$ the probability of a given event. In the remainder of this book, if no otherwise stated, we will focus on a scenario with equal a priori probabilities of the phenomenon, i.e., $p_0 = p_1 = 1/2$. However, similar results can be derived for a scenario with $p_0 \neq 1/2$. The sensors are clustered into $n_c < n$ groups, and each sensor can communicate only with its local first-level FC. The first-level FCs collect data from the sensors in their corresponding clusters and make local decisions on the status of the binary phenomenon. In a scenario with two levels of information fusion, each local FC transmits to the AP, which makes the final decision. A logical representation of this architecture is shown in Fig. 2.1.

The observed signal at the ith sensor[1] can be expressed as

$$r_i = c_E + n_i \quad i = 1, \ldots, n \tag{2.1}$$

where

$$c_E \triangleq \begin{cases} 0 & \text{if } H = H_0 \\ s & \text{if } H = H_1 \end{cases}$$

and $\{n_i\}$ are additive noise samples. Assuming that the noise samples $\{n_i\}$ are independent with the same Gaussian distribution $\mathcal{N}(0, \sigma^2)$, the common SNR at the sensors can be defined as follows:

$$\text{SNR}_{\text{sensor}} = \frac{[\mathbb{E}\{c_E|H_1\} - \mathbb{E}\{c_E|H_0\}]^2}{\sigma^2} = \frac{s^2}{\sigma^2}. \tag{2.2}$$

Each sensor makes a decision comparing its observation r_i with a threshold value τ_i and computes a local decision $u_i = U(r_i - \tau_i)$, where $U(\cdot)$ is the unit step

[1] Note that in this case we do not refer, for the ease of clearness, to the specific cluster, as done in Fig. 2.1. The particular situation will clarify the ambiguity.

function. In order to optimize the system performance, the thresholds $\{\tau_i\}$ need to be optimized. Even though, in general, a common value of the decision threshold for all sensors might not be the best choice, in the remainder of this chapter we assume that all sensors use the same decision threshold τ. While in a scenario with no clustering and ideal communication links between the sensors and the AP the relation between the optimized value of τ and s is well known [1], in the presence of clustering it is not. In the following, the value of τ will be optimized scenario by scenario. More precisely, we consider a possible (discrete) set of values which can be assumed by $\tau : \{\tau_{\min}, \tau_{\min} + \Delta\tau, \tau_{\min} + 2\Delta\tau, \ldots, \tau_{\max}\}$. In other words, τ can assume values in $[\tau_{\min}, \tau_{\max}]$ at regular steps of (sufficiently small) width $\Delta\tau$. For a given sensor SNR, the probability of decision error is evaluated for each possible value of τ, and the minimizing value is selected as threshold. In all considered cases, the optimized value of the common threshold is around $\sqrt{\text{SNR}_{\text{sensor}}}/2$, as already observed in [1, 2].

In a scenario with noisy communication links, modeled as Binary Symmetric Channels (BSCs), the decision u_i sent by the ith sensor can be *flipped* with a probability corresponding to the cross-over probability of the BSC model and denoted as p [3]. In general, a BSC might not be the best modelling choice for a wireless communication link, which might experience block fading [4–7]. However, in the presence of memoryless communication channels the use of a cross-over probability p is accurate. More precisely, p can be given a precise expression depending on the type of channel (with Additive White Gaussian Noise (AWGN) or bit-by-bit independent fading). Therefore, our simple model can give significant insights into the network behavior in many situations. The received bit at the fusion point (either an FC for clustered networks or directly the AP in the absence of clustering), referred to as $u_i^{(\text{r})}$, can be expressed as

$$u_i^{(\text{r})} = \begin{cases} u_i & \text{with probability } 1-p \\ 1-u_i & \text{with probability } p. \end{cases}$$

In the presence of noisy links, the value of the optimized local threshold τ, fixed for all sensors, might be different from that in a scenario with ideal communication links. As for the case with ideal communication links, this optimization will be carried out, for given SNR and clustering configuration, by minimizing the probability of decision error, as outlined at the end of the previous paragraph. Note that the best strategy would consist in using a properly optimized set of decision thresholds $\{\tau_i\}$ at the sensors. In particular, in a more general scenario where the type of event perceived by the sensor might vary, a more refined per-cluster optimization of the sensor decision threshold could be considered. However, since we are interested in monitoring a spatially constant binary phenomenon, we consider a simpler optimization approach, where the same threshold is used at all sensors.

While the communication links between sensors and first level FCs can be noisy, we assume that the other communication links in the network (i.e., from each FC to higher level FCs or the AP) are ideal. The rationale behind the assumption of ideal high-level links lies in the fact that in practical sensor network

design the FCs are likely to be placed relatively close to the AP. Therefore, under the assumption of a robust access control mechanism, one can assume that these links are ideal. The proposed analytical framework can be extended to encompass the presence of higher level noisy links. Moreover, realistic sensor network scenarios (with collisions) will be analyzed, through simulations and experiments, in Sect. 2.1.5.

We point out that the specific topologies of the considered networks are not explicitly taken into account. For instance, the distances between nodes are not explicitly mentioned. This corresponds to the assumption of modelling all noisy communication links as BSCs with the same cross-over probability. In order to extend our analytical framework, while still keeping the simple BSC-based link modelling, one can consider different cross-over probabilities (they could be associated with a specific network topology). This motivates the use of weighing fusion schemes, where the decisions to be fused together are weighed by the corresponding link qualities [8].

2.1.2 Analytical Framework

2.1.2.1 Uniform Clustering

In a scenario with *uniform* clustering, the sensors are grouped into identical clusters, i.e., each of the n_c clusters contains d_c sensors, with $n_c \cdot d_c = n$. A pictorial description of a uniformly clustered sensor network with $n = 16$ sensors and two decision levels is shown in Fig. 2.2: there are $n_c = 4$ clusters with $d_c = 4$ sensors each.

According to the assumption of majority-like information fusion considered in this chapter, the jth FC ($j = 1, \ldots, n_c$) computes a local decision using the following rule:

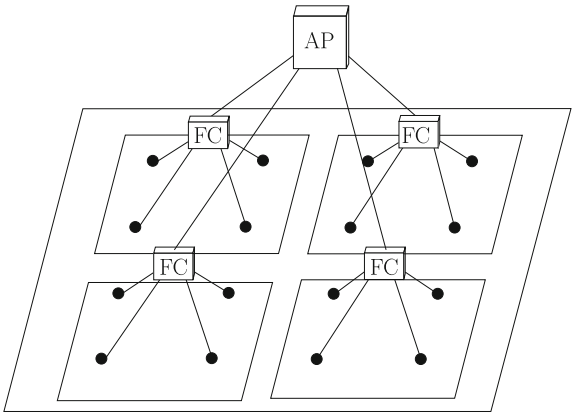

Fig. 2.2 An example of a uniformly clustered sensor network with $n = 16$ sensors. There are $n_c = 4$ clusters with $d_c = 4$ sensors each

$$\widehat{H}_j = \Gamma\left(u_1^{(j)}, \ldots, u_{d_c}^{(j)}\right) = \begin{cases} 0 & \text{if } \sum_{m=1}^{d_c} u_m^{(j)} < k \\ 1 & \text{if } \sum_{m=1}^{d_c} u_m^{(j)} \geq k \end{cases} \tag{2.3}$$

where $u_m^{(j)}$ is the mth decision of a sensor in the jth cluster and k is the FC decision threshold—since the clusters have the same dimension, the threshold $k = \lfloor d_c/2 \rfloor + 1$ is the same at all FCs. The AP decides with the following majority-like rule based on the local FC decisions $\{\widehat{H}_j\}$:

$$\widehat{H} = \Psi\left(\widehat{H}_1, \ldots, \widehat{H}_{n_c}\right) = \begin{cases} H_0 & \text{if } \sum_{j=1}^{n_c} \widehat{H}_j < k_f \\ H_1 & \text{if } \sum_{j=1}^{n_c} \widehat{H}_j \geq k_f \end{cases} \tag{2.4}$$

where $k_f = \lfloor n_c/2 \rfloor + 1$ is the fusion threshold at the AP. Using a combinatorial approach (based on the repeated trials formula [9]) and taking into account the decision rules (2.3) and (2.4), the probability of decision error at the AP can be expressed as follows:

$$\begin{aligned} P_e &= \mathbb{P}\{\widehat{H} = H_1 | H_0\}\mathbb{P}\{H_0\} + \mathbb{P}\{\widehat{H} = H_0 | H_1\}\mathbb{P}\{H_1\} \\ &= p_0 \, \mathrm{bin}(k_f, n, n_c, \mathrm{bin}(k, d_c, d_c, Q(\tau))) \end{aligned} \tag{2.5}$$

$$+ (1 - p_0) \, \mathrm{bin}(0, k_f - 1, n_c, (k, d_c, d_c, Q(\tau - s))) \tag{2.6}$$

where $Q(x) \triangleq \int_x^\infty \frac{1}{\sqrt{2\pi}} \exp(-y^2/2) \, \mathrm{d}y$ and

$$\mathrm{bin}(a, b, n, z) \triangleq \sum_{i=a}^{b} \binom{n}{i} z^i (1 - z)^{(n-i)} \tag{2.7}$$

where $a, b, n \in \mathbb{N}$ and $z \in (0, 1)$. If $n_c = k_f = 1$ and $d_c = n$, i.e., there is no clustering, and the probability of decision error (2.6) reduces to that derived in [3].

We point out that the majority fusion rule (2.3) with FC decision threshold $k = \lfloor d_c/2 \rfloor + 1$ is exact for *odd* values of k. For *even* values of k, the proposed fusion strategy tends to favor a final decision equal to '0.' For example, if $d_c = 2$, then only the received sequence 11 leads to a final decision in favor of '1.' However, since in all considered scenarios the two statuses of the binary phenomenon are equiprobable, setting k to $\lfloor d_c/2 \rfloor$ would unbalance the decision towards '1,' but, *on average*, the final performance would be the same.

Although we have previously derived the probability of decision error in a scenario with uniform clustering and two levels of information fusion, this analysis can be extended to a scenario with three levels of information fusion. In Fig. 2.3c, the logical structure of a sensor network with three decision levels is illustrated. For comparison, in the same figure the schemes with (a) no clustering and (b) two decision level uniform clustering are also shown. One should note that Fig. 2.3b is logically equivalent to the network schemes shown in Figs. 2.1 and 2.2. In a three decision level scenario the probability of decision error at the AP becomes

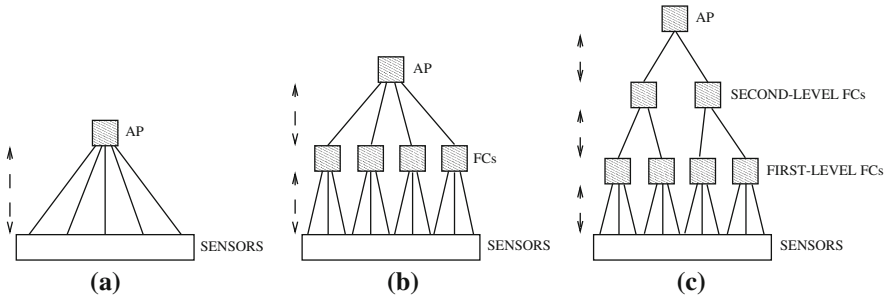

Fig. 2.3 Basic structures for sensor networks with distributed detection. Three cases are shown: **a** absence of clustering, **b** uniform clustering with two levels of information fusion, and **c** uniform clustering with three levels of information fusion

$$P_{\mathrm{e}} = p_0 \,\mathrm{bin}(k_{\mathrm{f}}, n_{\mathrm{c}_2}, n_{\mathrm{c}_2}, \mathrm{bin}(k_2, d_{\mathrm{c}_2}, d_{\mathrm{c}_2}, \mathrm{bin}(k_1, d_{\mathrm{c}_1}, d_{\mathrm{c}_1}, Q(\tau))))$$
$$+ (1 - p_0)\,\mathrm{bin}(0, k_{\mathrm{f}} - 1, n_{\mathrm{c}_2}, \mathrm{bin}(k_2, d_{\mathrm{c}_2}, d_{\mathrm{c}_2}, \mathrm{bin}(k_1, d_{\mathrm{c}_1}, d_{\mathrm{c}_1}, Q(\tau - s)))) \tag{2.8}$$

where n_{c_i} and d_{c_i} denote the number of clusters and nodes per cluster at the ith level ($i = 1, 2$), whereas k_i ($i = 1, 2$) is the majority-like fusion threshold at the ith level.

We remark that the above derivation can be straightforwardly extended to a scenario with a generic number of fusion levels. As for the scenario with uniform clustering and one decision level, the thresholds $\{k_i\}$ can be optimized by minimizing the probability of decision error at the AP.

2.1.2.2 Non-Uniform Clustering

Assuming a two-level sensor network topology, the probability of decision error in a generic scenario with non-uniform clustering can be evaluated as follows. Define the cluster size vector $\mathscr{D} \triangleq \{d_{\mathrm{c}}^{(1)}, d_{\mathrm{c}}^{(2)}, \ldots, d_{\mathrm{c}}^{(n_{\mathrm{c}})}\}$, where $d_{\mathrm{c}}^{(i)}$ is the number of sensors in the ith cluster ($i = 1, \ldots, n_{\mathrm{c}}$) and $\sum_{i=1}^{n_{\mathrm{c}}} d_{\mathrm{c}}^{(i)} = n$. Furthermore, define also the following two probability vectors:

$$\mathscr{P}^{\mathbf{1}|\mathbf{1}} \triangleq \left\{p_1^{1|1}, p_2^{1|1}, \ldots, p_{n_{\mathrm{c}}}^{1|1}\right\} \quad \mathscr{P}^{\mathbf{1}|\mathbf{0}} \triangleq \left\{p_1^{1|0}, p_2^{1|0}, \ldots, p_{n_{\mathrm{c}}}^{1|0}\right\}$$

where $p_\ell^{1|1}$ ($p_\ell^{1|0}$, respectively) is the probability that the ℓth FC decides for H_1 when H_1 (H_0, respectively) has happened. We still consider the use of a common threshold τ at the sensors, and its value is optimized as described in Sect. 2.1.1. The elements of $\mathscr{P}^{\mathbf{1}|\mathbf{1}}$ (equivalently, the elements of $\mathscr{P}^{\mathbf{1}|\mathbf{0}}$) are, in general, different from each other and depend on the particular distribution of the sensors among the clusters. In [8], it is shown that the probability of decision error can be expressed as follows:

$$P_{\mathrm{e}} = p_0 \sum_{i=k_{\mathrm{f}}}^{n} \sum_{j=1}^{\binom{n_{\mathrm{c}}}{i}} \prod_{\ell=1}^{n} \left\{ c_{i,j}(\ell) p_\ell^{1|0} + (1 - c_{i,j}(\ell))(1 - p_\ell^{1|0}) \right\}$$
$$+ (1 - p_0) \sum_{i=0}^{k-1} \sum_{j=1}^{\binom{n_{\mathrm{c}}}{i}} \prod_{\ell=1}^{n} \left\{ c_{i,j}(\ell) p_\ell^{1|1} + (1 - c_{i,j}(\ell))(1 - p_\ell^{1|1}) \right\} \quad (2.9)$$

where $\boldsymbol{c}_{i,j} = (c_{i,j}(1), \ldots, c_{i,j}(n_{\mathrm{c}}))$ is a vector which designates the jth configuration of the decisions from the first-level FCs in a case with i '1's (and, obviously, $n_{\mathrm{c}} - i$ '0's). In Table 2.1, the possible configurations of $\boldsymbol{c}_{i,j}$ are shown in the presence of $n_{\mathrm{c}} = 3$ clusters. For example, $\boldsymbol{c}_{1,2}$ is the second possible configuration with one '1' (and two '0'): the '1' is the decision of the second FC.

A scenario with *uniform* clustering can be interpreted as a special case of a generic non-uniform scenario. In this case, in fact, the elements of the three vectors $\mathscr{D}$, $\mathscr{P}^{\mathbf{1|1}}$, and $\mathscr{P}^{\mathbf{1|0}}$, become equal, i.e.:

$$\begin{cases} d_{\mathrm{c}}^{(i)} &= d_{\mathrm{c}} \\ p_i^{1|1} &= \mathrm{bin}(k, d_{\mathrm{c}}, d_{\mathrm{c}}, Q(\tau - s)) \\ p_i^{1|0} &= \mathrm{bin}(k, d_{\mathrm{c}}, d_{\mathrm{c}}, Q(\tau)) \end{cases}$$

$\forall i = 1, \ldots, n_{\mathrm{c}}$. It can be shown that (2.9) reduces to (2.6) in the presence of uniform clustering.

2.1.2.3 Scenarios with Noisy Communication Links

In a scenario with non-uniform clustering and two decision levels, the probability of decision error can be derived from (2.9), by replacing the probabilities $\{p_\ell^{1|i}\}_{\ell=1,\ldots,n_{\mathrm{c}}}^{i=0,1}$ with the probabilities $\{p_{\ell,\mathrm{noisy}}^{1|i}\}_{\ell=1,\ldots,n_{\mathrm{c}}}^{i=0,1}$, which take into account the noise in the communication links between sensors and FCs and are defined as follows:

Table 2.1 Possible configurations of $\boldsymbol{c}_{i,j}$ in a scenario with $n_{\mathrm{c}} = 3$ clusters

i	j	$\boldsymbol{c}_{i,j}$
0	1	000
	1	100
1	2	010
	3	001
	1	110
2	2	101
	3	011
3	1	111

$$p_{\ell,\text{noisy}}^{1|0}\left(d_{\text{c}}^{(\ell)}\right) = \sum_{m=k_\ell}^{d_{\text{c}}^{(\ell)}} \binom{d_{\text{c}}^{(\ell)}}{m} P_{10}^{m} P_{00}^{d_{\text{c}}^{(\ell)}-m} \tag{2.10}$$

$$p_{\ell,\text{noisy}}^{1|1}\left(d_{\text{c}}^{(\ell)}\right) = \sum_{m=k_\ell}^{d_{\text{c}}^{(\ell)}} \binom{d_{\text{c}}^{(\ell)}}{m} P_{11}^{m} P_{01}^{d_{\text{c}}^{(\ell)}-m} \tag{2.11}$$

where k_ℓ depends on the number of packets received at the ℓth FC. Since the same majority-like fusion rule of the AP is applied to each FC, the same considerations given above for k_{f} still apply here for the value of k_ℓ.

In (2.10), $P_{10} = 1 - P_{00}$ is the probability that a sensor decision sent to an FC is in favor of H_1 when H_0 has happened and can be expressed, according to the BSC model for a noisy communication link, as

$$P_{10} = Q(\tau)(1-p) + [1 - Q(\tau)]p. \tag{2.12}$$

In fact, the first term at the right-hand side is obtained when there is an observation error but error-free communications, whereas the second term is obtained when there are error-free observations but communication errors. Similarly, in (2.11) $P_{11} = 1 - P_{01}$ represents the probability that a decision sent by a sensor to an FC is in favor of H_1 when H_1 has happened and can be given the following expression:

$$P_{11} = Q(\tau - s)(1-p) + [1 - Q(\tau - s)]p. \tag{2.13}$$

Finally, the probability of decision error in a scenario with noisy communication links becomes

$$\begin{aligned} P_{\text{e}} = {} & p_0 \sum_{i=k_{\text{f}}}^{n} \sum_{j=1}^{\binom{n_{\text{c}}}{i}} \prod_{\ell=1}^{n} \left\{ c_{i,j}(\ell) p_{\ell,\text{noisy}}^{1|0} + (1 - c_{i,j}(\ell))(1 - p_{\ell,\text{noisy}}^{1|0}) \right\} \\ & + (1-p_0) \sum_{i=0}^{k_{\text{f}}-1} \sum_{j=1}^{\binom{n_{\text{c}}}{i}} \prod_{\ell=1}^{n_{\text{c}}} \left\{ c_{i,j}(\ell) p_{\ell,}^{1|1} + (1 - c_{i,j}(\ell))(1 - p_{\ell,\text{noisy}}^{1|1}) \right\}. \end{aligned} \tag{2.14}$$

2.1.3 Communication-Theoretic Characterization

2.1.3.1 Ideal Communication Links

The analytical framework presented in Sect. 2.1.2 leads to a communication-theoretic characterization of the network performance in terms of probability of decision error at the AP as a function of the sensor SNR and the communication noise level.

In Fig. 2.4, the probability of decision error is shown, as a function of the sensor SNR, in the case with $n = 16$ sensors, considering two and three decision levels.

In the scenario with two decision levels, the following topologies are possible:

- 8-8 (2 clusters with 8 sensors each);
- 4-4-4-4 (4 clusters with 4 sensors each);
- 2-2-2-2-2-2-2-2 (8 clusters with 2 sensors each).

For a three decision level scenario, the following topologies are considered:

- 4-4-4-4/2-2 (4 first-level FCs, each connected with 4 sensors, and 2 second-level FCs, each connected with 2 first-level FCs);
- 2-2-2-2-2-2-2-2/4-4 (8 first-level FCs, each connected with 2 sensors, and 2 second-level FCs, each connected with 4 first-level FCs);
- 2-2-2-2-2-2-2-2/2-2-2-2 (8 first-level FCs, each connected with 2 sensors, and 4 second-level FCs, each connected with 2 first-level FCs).

Lines and symbols (circles, triangles, and stars) correspond to analytical and simulation results, respectively. For comparison, the probability of decision error with no clustering is also shown. We point out that the simulation results shown in Fig. 2.4 and those shown, in the following, in Fig. 2.5 are meant to verify the correctness of the analytical framework. In other words, these results are obtained by simulating systems which are identical to those behind the analytical models. Obviously, the agreement between analysis and simulations is perfect, as no approximations were included. In Sect. 2.1.5, instead, the presented simulation results will refer to realistic IEEE 802.15.4 networks.

In Fig. 2.4, only one curve is shown for the scenario with two levels of information fusion, since the performance curves associated with all possible configurations (i.e., 8-8, 4-4-4-4, 2-2-2-2-2-2-2-2) overlap. This implies that one can choose between a uniform network topology with a small number of large clusters and a uniform network topology with a large number of small clusters, still

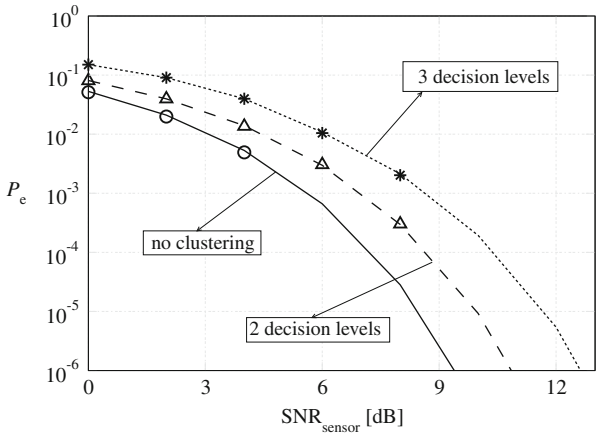

Fig. 2.4 Probability of decision error, as a function of the sensor SNR, in a scenario with $n = 16$ sensors and uniform clustering

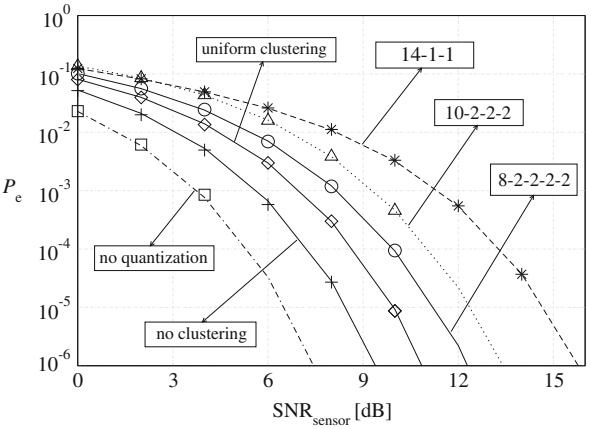

Fig. 2.5 Probability of decision error, as a function of the sensor SNR, in a scenario with $n = 16$ sensors. Various configurations are considered

guaranteeing the same performance level. The intuition behind this result is the following.

- If one considers an architecture with small clusters, then fusion at the first-level FCs is not effective. However, many local cluster decisions are then fused together, and this allows to recover (partially) the first-level information loss.
- On the other hand, considering large clusters leads to more reliable local first-level decisions. However, a few of them are then fused together, so that the supplementary (higher-level) refinement is not relevant.

Similar considerations also hold for a three decision level scenario. We point out that in Fig. 2.4 the obtained analytical expressions of the probability of decision error are numerically evaluated and verified through simulations.

Comparing the performance in the absence of clustering with that in the presence of uniform clustering (with either two or three decision levels), one can conclude that the larger is the number of decision levels, the worse is the performance. This is intuitive, since a larger number of decision levels corresponds to a larger number of partial information losses in correspondence to the fusion operations. However, this holds in scenarios with ideal communication links. In a wireless communication scenario, where some links may be completely obstructed, a sensor network with multiple communication layers might not yield the worst performance.

Although the analytical framework derived in the previous subsections is general, the presented results refer to networks with a (relatively) small number of sensors. However, our framework can be extended to scenarios with a large number of sensors. To this regard, in [8] a simple, yet very accurate, approximation of the derived framework, based on the application of the De-Moivre Laplace (DML) theorem, is proposed.

In order to evaluate the impact of non-uniform clustering, we consider a scenario with $n = 16$ sensors and various non-uniform network topologies. In Fig. 2.5, the

probability of decision error is shown, as a function of the sensor SNR, considering no clustering, two level uniform clustering, and various configurations with two decision levels and non-uniform clustering (explicitly indicated). For comparison, the curve in the absence of quantization at the sensors is also shown. The lines correspond to analytical results, whereas symbols are associated with simulations. In the scenarios with non-uniform clustering, the considered configurations are 8-2-2-2-2 (5 clusters, out of which 4 contain 2 nodes each and 1 contains 8 nodes), 10-2-2-2, and 14-1-1. As one can see from Fig. 2.5, in the presence of majority-like information fusion the higher is the non-uniformity degree among the clusters, i.e., the more unbalanced is clustering, the worse is system performance. Consequently, a sensor network designer should avoid non-uniform configurations with one big cluster and remaining small clusters. In general, a two-level uniformly clustered scenario is desirable, since it guarantees the smallest energetic loss with respect to a network with no clustering. However, uniform clustering in a realistic scenario might not be possible (e.g., in environmental monitoring applications). In fact, the area over which the sensors are distributed could be irregular and, therefore, uniform clustering of the sensors could not be feasible. An interesting application of our framework could consist in the identification of non-uniform clustering "classes," with similar performance per class. This could help significantly a network designer in predicting, for example, the performance degradation caused by the loss of some sensors (e.g., for battery exhaustion).

The above analysis in non-uniformly clustered scenarios applies to situations where the AP does not know the exact distribution of the sensors among the clusters. This is meaningful, for instance, in large networks where only local topology knowledge is possible. If, on the other hand, the distribution is very unbalanced (e.g., 14-1-1 with $n = 16$ sensors) and the AP knows the exact topology, the less reliable decisions originated by small clusters can be ignored. In a scenario with $n = 16$ sensors and the considered 14-1-1 topology, at $P_e = 10^{-4}$ a sensor SNR gain equal to 5.47 dB can be obtained without using, at the AP, the decisions associated with the smaller clusters—this corresponds to the performance of a sensor network with $n = 14$ sensors and no clustering. Therefore, knowledge of the clustering configuration at the AP allows to obtain a performance very close to that in the absence of clustering. In particular, in the previous case with $n = 16$ sensors and 14-1-1 configuration, the sensor SNR loss (with respect to a scenario with no clustering) can be reduced to 0.77 dB by using only the decision sent by the 14-sensor cluster. Our current focus, however, is on the comparison of clustering topologies when the AP gives the same weight to all received decisions. This is meaningful for a *dynamic* sensor network scenario, where sensors might die and sensors clusters might become unbalanced. In this case, intelligent reclustering techniques can be used to improve the system performance, as it will be shown in Sect. 2.2.

In Fig. 2.6, the probability of decision error is shown, as a function of the sensor SNR, for different values of the number of sensors n in a scenario with uniform clustering. In particular, the considered values for n are 16, 20, 32, 40, and 64. Observe that only one curve is associated with each value of n, since we have

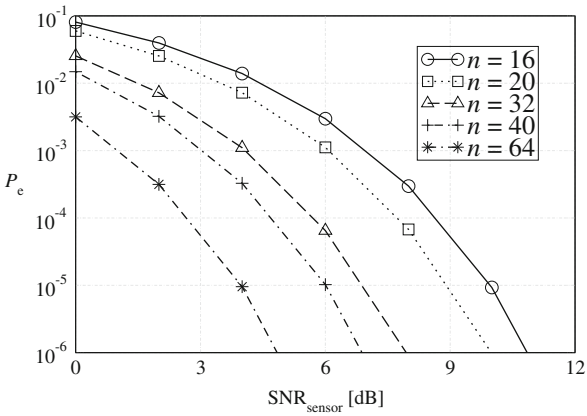

Fig. 2.6 Probability of decision error, as a function of the sensor SNR, in a scenario with uniform clustering. Different values of the number of sensors are considered

previously shown that the performance does not depend on the number of clusters (for a given n), as long as clustering is uniform. Obviously, the performance improves (i.e., the probability of decision error decreases) when the number of sensors in the network becomes larger. The results in Fig. 2.6 will be used in Sect. 2.2.1 to compute the sensor network lifetime under a QoS condition on the maximum acceptable probability of decision error.

2.1.3.2 Noisy Communication Links

While in Sect. 2.1.3.1 the performance in scenarios with ideal communication links has been analyzed, we now turn our attention to scenarios with noisy communication links. In particular, it is interesting to investigate how the probability of decision error behaves as a function of the communication noise level, i.e., the cross-over probability p. To this end, we introduce a communication-theoretic QoS condition, in terms of the maximum tolerable probability of decision error, denoted as P_e^*, at the AP. A physical layer-oriented QoS condition can be written as

$$P_e \leq P_e^*. \tag{2.15}$$

Since the probability of decision error is a monotonically decreasing function of the sensor SNR, the QoS condition (2.15) can be equivalently rewritten as

$$\mathrm{SNR}_{\mathrm{sensor}} \geq \mathrm{SNR}_{\mathrm{sensor}}^*$$

where $\mathrm{SNR}_{\mathrm{sensor}}^*$ depends on P_e^*. It is then possible to evaluate the performance under a desired QoS constraint, given by the maximum tolerable probability of decision error P_e^*.

In Fig. 2.7, the value of the minimum sensor SNR required to guarantee P_e^*, i.e., $\mathrm{SNR}_{\mathrm{sensor}}^*$, is shown, as a function of the cross-over probability p, in scenarios (i) without clustering and (ii) with clustering and two decision levels, respectively. Two possible values for P_e^* are considered: (i) 10^{-3} (curves with circles) and (ii) 10^{-4} (curves with triangles). As expected, when the noise level increases, the minimum

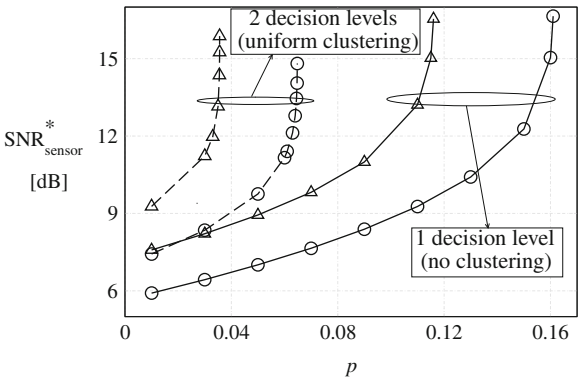

Fig. 2.7 Minimum sensor SNR required to obtain a desired QoS, in scenarios with noisy communication links in the cases (i) without clustering and (ii) with uniform clustering and two decision levels. Two possible QoS conditions are considered: (i) $P_e^* = 10^{-3}$ (*lines with circles*) and (ii) $P_e^* = 10^{-4}$ (*lines with triangles*)

sensor SNR required to guarantee the desired network performance also increases. In fact, since communications become less reliable, a higher accuracy in the observation phase is needed in order to maintain the same overall performance. Besides, one can observe that there exists a vertical asymptote in each curve in Fig. 2.7. In other words, there exists a critical value p_{crit} of the noise level, such that: (i) for $p < p_{\text{crit}}$, the sensor network is operative, i.e., there exists a finite value of the sensor SNR which satisfies the desired QoS condition (2.15); (ii) for $p > p_{\text{crit}}$, instead, the network is not operative, i.e., it is not possible to achieve the desired performance level, *regardless* of the value of the sensor SNR. One could equivalently describe this behavior as *bimodal*. This is a typical behavior of distributed communication networks, such as the bimodal connectivity behavior in ad hoc wireless networks [10–14]. Proper operation of the considered sensor networks with distributed detection can be equivalently interpreted as a symptom of network connectedness. In Fig. 2.7, this bimodal behavior is also confirmed in a scenario with uniform clustering and two decision levels. However, in the latter case the impact of the communication noise is stronger with respect to a scenario with no clustering, i.e., the network looses connectivity for smaller values of p. Consequently, the larger is the number of decision levels in the network, the lower is the maximum tolerable communication noise level.

2.1.4 Joint Communication/Information-Theoretic Characterization

The considered sensor network schemes can be modeled as "black boxes" with a binary input (the phenomenon H) and a binary output (the decision $\widehat{H}$ at the AP). Using the model in Fig. 2.1, the final decision $\widehat{H}$ can be described as a binary random variable[2] with $P_0 \triangleq P(\widehat{H} = H_0)$. In a scenario with two-level uniform

[2] Note that the definition of $P_0 = \mathbb{P}\{\widehat{H} = H_0\}$ (relative to the decision $\widehat{H}$) is different from that given for the *a priori* probability of the phenomenon $p_0 = \mathbb{P}\{H = H_0\}$ given in Sect. 2.1.1.

clustering and ideal communication links, the parameter P_0 can be rewritten (using the results in Sect. 2.1.1) as

$$P_0 = p_0 \,\mathrm{bin}(0, k_\mathrm{f} - 1, n_\mathrm{c}, \mathrm{bin}(k, d_\mathrm{c}, d_\mathrm{c}, Q(\tau))) + (1 - p_0)\,\mathrm{bin}(0, k_\mathrm{f} - 1, n_\mathrm{c}, \mathrm{bin}(k, d_\mathrm{c}, d_\mathrm{c}, Q(\tau - s))). \tag{2.16}$$

We remark that Eq. 2.16 may look identical to (2.6). In (2.16), however, the term on the right-hand side in the first row corresponds to $\mathbb{P}\{\widehat{H} = H_0|H_0\}$, whereas in (2.6) it is given by $\mathbb{P}\{\widehat{H} = H_1|H_0\}$—the second parameter of the function "bin" is, in fact, different in the two cases.

The mutual information of the Binary Input Binary Output (BIBO) sensor network can then be written as [15, Chap. 2]

$$I(H; \widehat{H}) = H_\mathrm{e}(\widehat{H}) - H_\mathrm{e}(\widehat{H}|H)$$

where $H_\mathrm{e}(\cdot)$ is the entropy of a random variable; in particular, $H_\mathrm{e}(\widehat{H}|H)$ is the conditional entropy of $\widehat{H}$ given H [15]. After a few manipulations, the mutual information becomes

$$I(H; \widehat{H}) = H_\mathrm{e}(p_0(1 - p_{10}) + (1 - p_0)p_{01}) - p_0 H_\mathrm{e}(p_{10}) - (1 - p_0)H_\mathrm{e}(p_{01}) \tag{2.17}$$

where $p_{ij} \triangleq \mathbb{P}\{\widehat{H} = H_i|H_j\}$, $i, j = 0, 1$.

In Fig. 2.8, the probability of decision error is shown, as a function of the *mutual information*, for the same scenario considered in Fig. 2.5, i.e., with no clustering (circles), uniform clustering (triangles), and non-uniform clustering (pluses, 14-1-1 configuration), respectively. The communication links are ideal. The curves considered in this figure are parameterized curves, obtained by

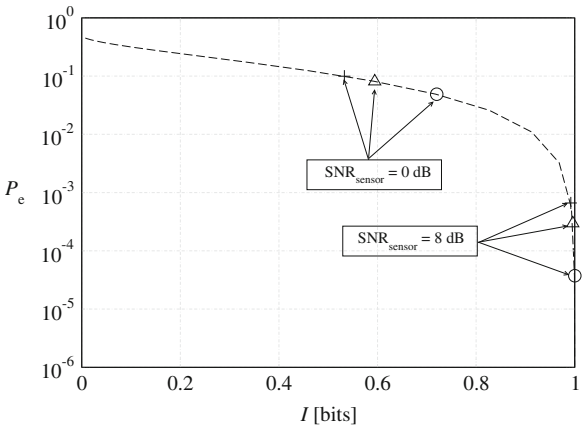

Fig. 2.8 Probability of decision error, as a function of the mutual information, in a scenario with $n = 16$ sensors. The operating points for various clustering configurations and two sensor SNRs are shown

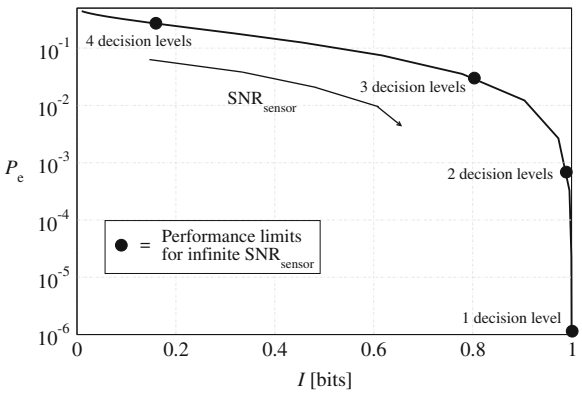

Fig. 2.9 Probability of decision error, as a function of the mutual information, in a scenario with $n = 16$ sensors, uniform clustering, and noisy communication links ($p = 0.05$)

combining probability of decision error curves with mutual information curves, through the common parameter given by the sensor SNR. As one can see, the curves associated with different sensor network topologies overlap. In other words, for a given value of the mutual information, the probability of decision error is fixed. Note, however, that a specific mutual information is obtained in clustered (for example, 4-4-4-4 or 2-2-2-2-2-2-2-2) and non-clustered scenarios for different values of the sensor SNR (in the figure, a few representative points associated with two SNRs are highlighted). This means that, for a given mutual information, the presence of clustering leads to an *energetic loss* at the sensors (in the observation phase). The loss with non-uniform clustering is higher than with uniform clustering. Similar curves can be derived for the other scenarios considered in this chapter, e.g., for a large number of sensors, with more than two decision levels, and in the presence of noisy communication links between sensors and first-level FCs (with sufficiently low values of the noise level p). However, the network behavior does not change, i.e., for a fixed value of the mutual information, the probability of decision error is uniquely determined.

In Fig. 2.9, the probability of decision error is shown, as a function of the mutual information, in a scenario with $n = 16$ sensors and uniform clustering. Communication links between sensors and first-level FCs are noisy, with cross-over probability $p = 0.05$. The limiting (for $\mathrm{SNR}_{\mathrm{sensor}} \to \infty$) operating points over the $P_e - I$ curve of a BIBO sensor network, corresponding to all possible numbers of decision levels (1–4, respectively), are shown. For a given number of decision levels, the system operating point moves from the position corresponding to $I = 0$ (for very low values of $\mathrm{SNR}_{\mathrm{sensor}}$) to the corresponding limiting point, which is asymptotically approached for $\mathrm{SNR}_{\mathrm{sensor}} \to \infty$. As one can see, the presence of noise over the communication links limits the maximum achievable mutual information, i.e., the maximum information transfer rate across the network.

In [16], possible simplified expressions for the probability of decision error (as a function of the mutual information) are presented. In particular, (i) polynomial approximations, (ii) asymptotic (for sufficiently large sensor SNR) analytical expressions, and (iii) *bimodal* approximations (valid for all sensor SNRs) are derived.

2.1.5 Realistic Clustered Networks with Data Fusion

In this subsection, we present *simulation* and *experimental* results which validate our analytical framework on distributed detection in practical sensor networking scenarios, where nodes comply with the IEEE 802.15.4 standard.

2.1.5.1 Simulations

The simulations have been carried out with the Opnet Modeler simulator [17] and a built-in IEEE 802.15.4 network model designed at the National Institute of Standards and Technologies (NIST) [18]. This model provides only the first two layers of the ISO/OSI stack, and we have extended it with a simple Opnet model for a FC, which, in addition to providing relaying functionalities, implements the intermediate data fusion mechanisms described in the previous subsections. Our Opnet model assumes strong line-of-sight communications between the sensors and the FCs, and between the FCs and the coordinator.

According to the theoretical analysis, the sensors make a noisy observation (affected by AWGN) of a randomly generated binary phenomenon H and make local decisions on the status of the phenomenon. Subsequently, the sensors embed their decisions into proper data packets of length 216 bits,[3] which are sent either to the coordinator (in the absence of clustering) or to the first-level FCs (in the presence of clustering). The decisions are assumed to be either 0 (no phenomenon) or 1 (presence of the phenomenon). Obviously, if some packets are lost due to medium access collisions, decisions (either at the FCs or at the AP) are made only on the basis of the received packets (this leads to a reduced reliability of the decisions). If all the packets related to a set of observations of the same phenomenon are lost, instead, the final binary decision is random. Finally, if half of the decisions are in favor of one phenomenon status and the other half are in favor of the other, the coordinator decides for the presence of the phenomenon. More details about the implementation of the data fusion mechanism in Opnet can be found in [19].

[3] This length corresponds to a payload of 96 bits and a header of 120 bits introduced by physical and MAC layers.

In both scenarios, it is possible to evaluate, by simulation, the probability of decision error. Together with the probability of decision error, the simulator allows to evaluate (i) the *packet delivery fraction*, denoted as ξ and defined as the ratio between the number of packets correctly delivered at the coordinator and the number of packets sent by the sensors, and (ii) the *delay*, defined as the time interval between the transmission instant and the reception instant of a generic packet. Results about the aggregate throughput [dimension: (pck/s)], defined as $S_{\text{agg}} = n \cdot g \cdot \xi$, where n is the number of transmitting sensors and g is the packet generation rate (set to 2 pck/s in all simulation results presented in the remainder of this subsection), can be found in [19]. Moreover, no acknowledgement (ACK) messages are used to confirm successful transmissions. In order to eliminate possible statistical fluctuations, each simulation performance point is obtained by averaging the results of ten Opnet simulation runs.

In Fig. 2.10, the packet delivery fraction and the delay are shown as functions of the number n of transmitting sensors. These curves are obtained considering a fixed observation SNR at the sensors (equal to 0 dB). Our results, however, show that the packet delivery fraction and the delay are not affected by the value of the observation SNR at the sensors. We consider, in fact, ideal communication channels, so that only the observations at sensors are noisy, whereas the packets sent from the sensors to either an FC (clustered schemes) or the coordinator (non-clustered schemes) are received without errors. Consequently, the performance does not depend on the considered SNR, since packet delivery fraction and delay are network performance indicators and do not depend on the observation reliability. The packet delivery fraction (solid line with circles) decreases monotonically. In particular, for small values of n, it remains close to 1. When the number of transmitting nodes increases, instead, the number of collisions in the channel increases as well, and the packet delivery fraction reduces. In the same figure, the delay (dotted line with diamonds) is also shown. As the intuition suggests, the delay is short for small values of n. When the traffic

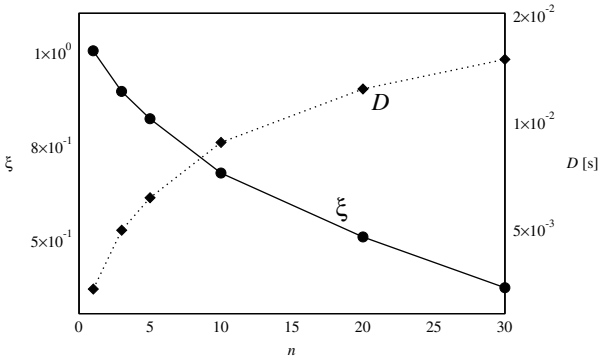

Fig. 2.10 Performance analysis in a scenario without clustering: packet delivery fraction and delay performance as functions of the number n of transmitting sensors

increases, instead, due to a larger number of collisions, the delay is longer, since the channel is busy for a longer period of time and the probability of finding the channel idle reduces. Finally, for large values of n, the delay seems to start saturating to a maximum value. In this case, in fact, due to the increased offered traffic, at least one sensor is likely to be ready to send its packet as soon as the channel becomes idle.

In Fig. 2.11, we analyze the impact of non-uniform clustering on the probability of decision error—as a performance benchmark, the probability of decision error in the case with uniform clustering is also shown. We consider scenarios with $n = 16$ sensors and the following network configurations: (i) no clustering, (ii) 8-8, (iii) 4-4-4-4 FCs, (iv) 14-1-1, (v) 10-2-2-2, and (vi) 8-2-2-2-2. According to the results in Fig. 2.11, the best performance is obtained in the absence of clustering, whereas the worst performance is obtained in the 14-1-1 scenario, i.e., with 3 FCs and non-uniform clustering. From Fig. 2.11, one can conclude that, in the presence of non-uniform clustering, the performance improves for relatively balanced clusters (as also predicted by the analytical framework). In this case, in fact, decisions made by intermediate FCs are more reliable, so the final decision made by the coordinator is more likely to be correct. In the case of uniform clustering, instead, the probability of decision error is *not* affected by the number of clusters in the network, as long as the total number of sensors remains the same: observing Fig. 2.11, one can note that the curves relative to the scenarios with four 4-sensor clusters and two 8-sensor clusters are almost overlapped. This is due to the fact that a smaller number of clusters is compensated by a higher quality of the intermediate decisions. This result is in agreement with the theoretical conclusions reached in Sect. 2.1.3.1. However, note that the performance in IEEE 802.15.4 scenarios worsens with respect to the analytical case, because the simulator takes into account the losses due to collisions. Since some packets may be lost, the probability of decision error is influenced by the collisions.

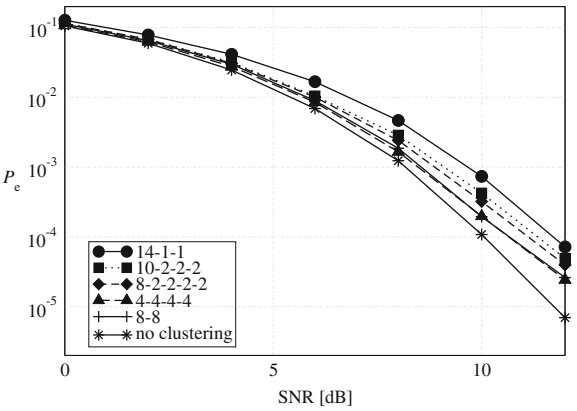

Fig. 2.11 BER performance in scenarios with $n = 16$ sensors both in the case of uniform and non-uniform clustering. Various topologies (indicated in the figure) are considered

2.1.5.2 Experiments

In order to verify the predictions of the theoretical framework from an experimental perspective, we consider a networking set-up formed by MicaZ nodes [20]. MicaZ platforms include an ATmega128L 7.3 MHz micro-controller [21], FLASH and EEPROM memories, and a 2.4 GHz IEEE 802.15.4 Chipcon CC2420 radio-frequency transceiver [22]. The nodes' operating system is TinyOS. The experimental set-up is characterized by $n = 16$ nodes, organized in uniform clusters, with two and three decision levels, respectively. In our implementation, each node observes a "0" phenomenon and adds a Gaussian observation noise generated through the function "random" available in the TinyOS environment. According to the local decision threshold, each source node makes a decision on the observed phenomenon and embeds it in a packet to be transmitted. Since each TinyOS packet is formed by a payload of 30 bytes (the first byte contains the dimension and the following 29 the information data), we embed in each packet $29 \times 8 = 232$ consecutive binary decisions. This corresponds to 232 consecutive (time-wise) realizations of the observed binary phenomenon. The packets originated by the source nodes are then transmitted, through the intermediate FCs, to the AP. Note that a packet duration is of the order of 1 ms, and consecutive packet transmissions are separated by approximately 0.1 s. The transmit power is set to -25 dBm and the sensitivity threshold at the receivers is -100 dBm. The distances between communicating nodes (of the order of 2 m) are such that the received power is significantly higher than the sensitivity threshold. The data fusion mechanisms at the intermediate FCs and at the AP follows the majority decision rules described in the analytical framework.

The experimental Bit Error Rate (BER) performance is shown in Fig. 2.12. In the same figure, for comparison, we also show the corresponding theoretical results extracted from Fig. 2.4. As one can see, the experimental results are slightly worse than the theoretical ones (as observed also, in Sect. 2.1.5.1 for

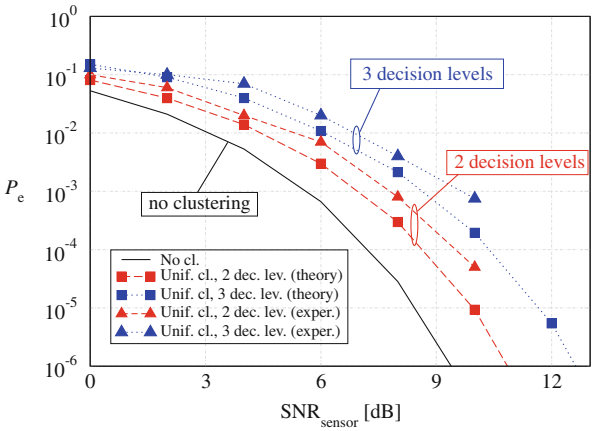

Fig. 2.12 Experimental BER performance in scenarios with $n = 16$ sensors and uniform clustering. Two and three decision levels are considered

simulation results), but confirm the trend. This discrepancy is due to the more realistic experimental scenario, where some packets may get lost because of the wireless communication links. Since the decision rules at the FCs and at the AP do not adapt to the number of received observations, this explains the performance degradation. We point out that in our experiments the packet losses are typically *not* due to collisions, i.e., the traffic load of the considered network scenarios is too low to create problems at the access level. On the opposite, the performance degradation is due to losses of packets due to propagation reasons.

2.2 Extending the Lifetime of Clustered Sensor Networks

2.2.1 Sensor Network Lifetime under a Physical Layer QoS Condition

In order to evaluate the sensor network lifetime, one needs first to define when the network has to be considered "alive." We assume that the network is "alive" until the QoS condition in (2.15) is satisfied. When a sensor in the network dies (e.g., there is a hardware failure or its battery exhausts), the probability of decision error increases since a smaller number of sensors is alive (see, for instance, Fig. 2.6). Moreover, the presence of a specific clustering configuration might make the process of network death faster. More precisely, the network dies when the desired QoS condition (2.15) is no longer satisfied, as a consequence of the death of a *critical sensor*. Therefore, the network lifetime corresponds to the lifetime of this critical sensor. Obviously, the criticality of a sensor's death depends on the particular sequence of previous sensors' deaths.

On the basis of the considerations in the previous section, in order to estimate the *network* lifetime one, first, needs to consider a reasonable model for the *sensor* lifetime. We denote by $F(t) \triangleq \mathbb{P}\{T_{\text{sensor}} \leq t\}$ the Cumulative Distribution Function (CDF) of a sensor's lifetime T_{sensor} (the same for all sensors) and we consider the following exponential distribution as representative:

$$F(t) = \left[1 - \mathrm{e}^{-t/\mu}\right] U(t) \tag{2.18}$$

where μ is the mean of the exponential distribution, the time t is measured in arbitrary units [dimension: (aU)]. We have chosen the distribution in (2.18) as a good model for a sensor lifetime [23, Ch. 8]. Note that the results presented here for an exponential distributions also hold for other sensor lifetime distributions [24].

As mentioned before, we are interested in analyzing the network behavior when the QoS condition (2.15) is satisfied. More precisely, in the following subsections we evaluate the sensor network lifetime in scenarios with (A) ideal reclustering and (B) no reclustering. The obtained results are then commented.

2.2.1.1 Analysis with Ideal Reclustering

In the case of *ideal reclustering*, the network dynamically reconfigures its topology, immediately after a sensor death, in order to recreate a uniform configuration. Obviously, the time needed for rearranging the network topology depends on the specific strategy chosen in order to reconfigure correctly (according to the updated network configuration) the connections between the sensors and the FCs and those between the FCs and the AP. In Sect. 2.2.2, a simple reconfiguration strategy will be proposed.

Given a maximum tolerable probability of decision error P_e^*, one can determine the smallest number of sensors, denoted as $n_{\min}$, required to satisfy the desired QoS condition. For instance, considering Fig. 2.6 and fixing a maximum tolerable value P_e^*, one can observe that, for decreasing numbers of sensors, at some point the actual probability of decision error P_e becomes higher than P_e^*. In other words, the probability of decision error is lower than P_e^* if *at least* $n_{\min}$ sensors are alive or, equivalently, until $n_{\text{crit}} = n - n_{\min} + 1$ sensors die. Therefore, denoting as T_{net} the network lifetime, one can write:

$$\mathbb{P}\{T_{\text{net}} \leq t\} = \mathbb{P}\{\text{at least } n_{\text{crit}} \text{ sensors have } T_{\text{sensor}} < t\}$$

where T_{sensor} is the sensor lifetime (recall that this random variable has the same distribution for all sensors) with CDF $F(t)$. Since the lifetimes of different sensors are assumed independent, using the repeated trials formula, one obtains

$$\mathbb{P}\{T_{\text{net}} \leq t\} = \sum_{i=n_{\text{crit}}}^{n} \binom{n}{n_{\text{crit}}} [F(t)]^i [1 - F(t)]^{n-i}.$$

2.2.1.2 Absence of Reclustering

In the previous subsection, we have analyzed the network evolution in an ideal scenario where the topology is dynamically reconfigured in response to a sensor death (e.g., because of the depletion of its battery or hardware failure). However, it might happen that the initial clustered configuration is fixed, i.e., the connections between sensors, FCs, and AP cannot be modified after a sensor death. In this case, the following question is relevant: is there an optimum initial topology which leads to longest network lifetime? In order to answer this question, we will analyze the network evolution in scenarios where there is no reclustering. The network is still considered dead when the QoS condition (2.15) is no longer satisfied.

In the absence of ideal reclustering, an analytical performance evaluation is not feasible, i.e., there does not exist a closed-form expression for the CDF of the network lifetime. In fact, the CDF depends on the particular network evolution, i.e., it depends on how the sensors die among the clusters in the network. Therefore, each sequence of sensors' deaths is characterized by a specific lifetime, and one needs to resort to simulations in order to extrapolate an average statistical characterization. The simulations are performed according to the following steps.

1. The lifetimes of all n sensors are generated according to the chosen distribution and the sensors are randomly assigned to the clusters.
2. The sensors' lifetimes are ordered in an increasing manner.
3. After a sensor death, the network topology is updated.
4. The probability of decision error is computed in correspondence to the surviving topology determined at the previous point: if the QoS condition (2.15) is satisfied, then the evolution of the network continues from step 3, otherwise, step 5 applies.
5. The network lifetime corresponds to the lifetime of the last dead sensor.

In Fig. 2.13, the CDF of the network lifetime is shown, as a function of time, in a scenario with $n = 32$ sensors grouped, respectively, in 2, 4, and 8 clusters. The sensor SNR is set to 5 dB and the maximum tolerable probability of decision error is $P_e^* = 10^{-3}$. For comparison, the curve associated with ideal reclustering is also shown. One can observe that the larger is the number of clusters, the worse is the performance, i.e., the higher is the probability of network death. Moreover, the curve associated with two clusters is very close to that relative to ideal reclustering. In fact, in a scenario with only two clusters, the average number of sensors which die in each cluster is approximately the same and, consequently, the topology remains approximatively uniform.

In Table 2.2, the network lifetime corresponding to a CDF equal to 0.9 (i.e., an outage probability of 90%) is shown, assuming an *exponential* sensor lifetime (with $\mu = 1$ aU), for various clustering configurations and values of the maximum tolerable probability of decision error P_e^*. The number of sensors is $n = 64$. For comparison, the network lifetime with ideal reclustering is also shown. From the results in Table 2.2, the following observations can be carried out.

- For a small number of clusters (2 or 4), the lifetime reduction, with respect to a scenario with ideal reclustering, is negligible. This is to be expected from the results in Fig. 2.13 and is due to the fact that the sensors die "more or less"

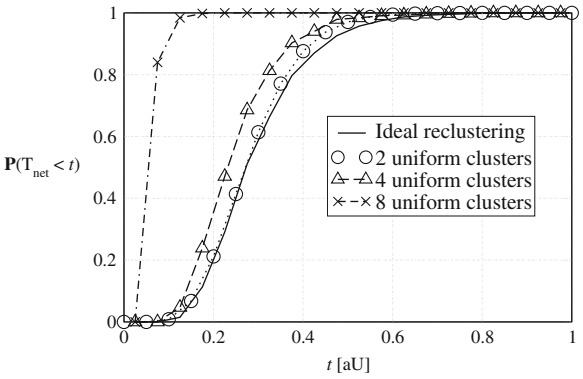

Fig. 2.13 CDF of the network lifetime, as a function of time, in a scenario with $n = 32$ sensors, uniform clustering (with, respectively, 2, 4, and 8 clusters), and *absence of reclustering* (simulation results). The sensor SNR is set to 5 dB and the maximum tolerable probability of decision error is $P_e^* = 10^{-3}$. For comparison, the curve associated with ideal reclustering (analytical results) is also shown

Table 2.2 Sensor network lifetime corresponding to an outage probability equal to 90% in a scenario with $n = 64$ sensors and $\text{SNR}_{\text{sensor}} = 5$ dB. Three values for the maximum tolerable probability of decision error P_e^* are considered: (i) 10^{-2}, (ii) 10^{-3}, and (iii) 10^{-4}. The mean parameter of the exponential distribution is $\mu = 1$ aU. All time values in the table entries are expressed in aU

P_e^*	Ideal reclustering	No reclustering (2 clusters)	No reclustering (4 clusters)	No reclustering (8 clusters)
10^{-2}	2.1	2.1	2.0	1.68
10^{-3}	1.3	1.3	1.2	1.012
10^{-4}	0.78	0.78	0.74	0.725

uniformly in all clusters. When the number of clusters increases beyond 4, the network lifetime starts to reduce appreciably. Therefore, our results show that, in the *absence of ideal reclustering*, the winning strategy to prolong network lifetime is to *form a few large clusters*.

- The impact of the QoS condition is very strong. In fact, when the QoS condition becomes more stringent (i.e., P_e^* decreases), the network lifetime shortens, since a smaller number of sensor deaths is sufficient to violate this condition. On the other hand, if the QoS condition is less stringent, then a larger number of sensors have to die in order to violate it.
- The impact of the number of nodes on the network lifetime has not been directly analyzed. However, since the performance improves when the number of sensors increases (as shown in Fig. 2.6), one can conclude that, for a fixed QoS condition, a network with a larger number of sensors will satisfy the QoS condition for a longer time and, therefore, the network lifetime will be prolonged. Equivalently, one can impose a stronger QoS condition (a lower value of P_e^*), still guaranteeing the same network lifetime.

2.2.2 Analytical Computation of Network Lifetime

In Sect. 2.2.1, we have analyzed the network performance without taking into account the *cost* of reclustering. In this subsection, instead, we investigate, from an analytical viewpoint, the cost of the used reclustering protocol in terms of its impact on the sensor network lifetime. In order to evaluate the cost of reclustering, one first needs to detail a reclustering protocol. We remark that we limit ourselves mainly (but not only) to scenarios with two (big) clusters, since they are associated with the minimum loss, in terms of probability of decision error at the AP, with respect to the scenario with the absence of clustering.

The reclustering protocol which will be used can be characterized as follows.

1. When an FC senses that a sensor belonging to its cluster is dead, e.g., when it does not receive packets from this sensor, it sends a control message, referred to as "ALERT," to the AP.

2. Assuming that the AP is aware of the current network topology, when it receives an ALERT message, it decides if reclustering has to be carried out. If so, the optimized network topology is determined.
3. If no reclustering is required, the AP sends to both FCs an "OK" message to confirm the current topology. On the other hand, if reclustering has to be carried out, another message, referred to as "CHANGE" and containing the new topology information, is sent to the FCs. In the latter case, the FCs send the CHANGE message also to sensors in order to allow them to communicate with the correct FC from then on.
4. If reclustering has happened, the sensors retransmit their previous packet to the FCs according to the new topology and a new data fusion is carried out at the AP.

In Fig. 2.14, the behavior of this simple protocol is pictured in an illustrative scenario with $n = 11$ sensors and two clusters (with 6 and 5 sensors, respectively). The control messages associated with solid lines are exchanged in the absence of reclustering, whereas the messages associated with dashed lines are exchanged in the presence of reclustering.

In order to derive a simple analytical framework for evaluating the sensor network lifetime, the following assumptions are expedient.

(a) The observation frequency, referred to as f_{obs}, is sufficiently low to allow regular transmissions from the sensors to the AP and, if necessary, the applicability of the reclustering protocol (this is reasonable for scenarios where the status of the observed phenomenon does not change rapidly).
(b) Transmissions between sensors and FCs and between FCs and AP are supposed instantaneous (this is reasonable, for example, if FCs and AP are connected through wired links or very reliable wireless links).
(c) Data processing and topology reconfiguration are instantaneous (this is reasonable if the processing power at the AP is sufficiently high).
(d) There is perfect synchronization among all nodes in the network (this is a reasonable assumption if nodes are equipped with synchronization devices, e.g., global positioning system).

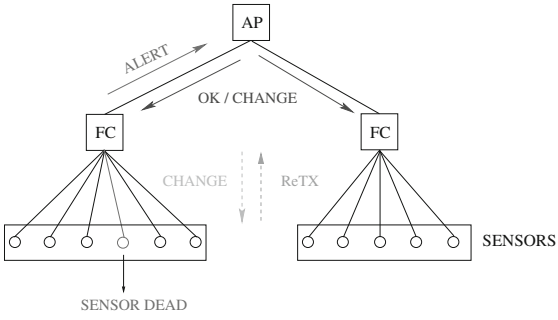

Fig. 2.14 Message exchange in the proposed reclustering protocol. A network scenario with $n = 11$ sensors and two clusters (with 6 and 5 sensors, respectively) is considered. The control messages evolution follows the death of a sensor

The proposed reclustering algorithm and the assumptions above might look too simplistic for a realistic wireless sensor network scenario. However, they allow to obtain significant insights about the cost, in terms of network lifetime, of adaptive reclustering.

We preliminary assume that the duration of a data packet transmission has no influence on the lifetime of a single sensor—a more accurate analysis, which takes properly into account the actual duration of a data transmission, will be proposed in Sect. 2.2.4. In this case, the network lifetime can be written as

$$T_{\text{net}} = \sum_{i=1}^{n_{\text{crit}}} T_{\text{d},i}$$

where n_{crit} has been introduced in Sect. 2.2.1.1 and $T_{\text{d},i}$ is the time interval between the $(i-1)$th sensor death and the ith sensor death. Obviously, $T_{\text{d},1}$ is the time interval until the death of the first sensor and can be written as

$$T_{\text{d},1} = \min_{j=1,\ldots,n} \{T_j\} \tag{2.19}$$

where T_j is the lifetime of the jth sensor. Since T_{net} is a r.v., one could determine its statistics (e.g., the CDF). However, in order to concisely characterize the impact of reclustering, it is of interest to evaluate its average value, i.e.,

$$\mathbb{E}[T_{\text{net}}] = \mathbb{E}\left[\sum_{i=1}^{n_{\text{crit}}} T_{\text{d},i}\right]. \tag{2.20}$$

2.2.2.1 Absence of Reclustering

In this case, n_{crit} and $\{T_{\text{d},i}\}$ in (2.20) are independent r.v.s. In fact, they depend on the sensors' lifetime distribution and on the particular evolution (due to the nodes' deaths) of the network topology. Therefore, the sum in (2.20) is a stochastic sum. Using the conditional expectation theorem and the fundamental theorem of probability [9], one can write

$$\mathbb{E}\left[\sum_{i=1}^{n_{\text{crit}}} T_{\text{d},i}\right] = \sum_{j=1}^{n} \mathbb{P}\{n_{\text{crit}} = j\} \sum_{i=1}^{j} \mathbb{E}\left[T_{\text{d},i}\right].$$

At this point, one needs to resort to simulations to compute the probabilities $\{P(n_{\text{crit}} = j)\}$. In fact, they strongly depend on the particular network evolution before its death.

2.2.2.2 Ideal Reclustering

In Sect. 2.2.1, we have shown that the presence of ideal reclustering leads to an upper bound on the network lifetime, i.e., it tolerates the maximum number of

sensors' deaths before the network dies. This bound can be analytically evaluated using (2.20) and replacing n_{crit} with the value $n_{\text{crit}}^{\text{R}}$ defined as follows:

$$n_{\text{crit}}^{\text{R}} = \min_{n_{\text{crit}}^{*}=1,\ldots,n} \{P_{\text{e}}(\text{after } n_{\text{crit}}^{*} \text{ sensors' deaths}) \geq P_{\text{e}}^{*}\}.$$

The value of $n_{\text{crit}}^{\text{R}}$ can be determined by numerical inversion of the QoS condition. Therefore, an upper bound for the network lifetime can be expressed as

$$\text{UB}_{T_{\text{net}}} \triangleq \mathbb{E}\left[T_{\text{net}} | n_{\text{crit}} = n_{\text{crit}}^{\text{R}}\right] = \sum_{i=1}^{n_{\text{crit}}^{\text{R}}} \mathbb{E}\left[T_{\text{d},i}\right]. \tag{2.21}$$

In this case, one can observe that the sum in (2.21) is deterministic and, therefore, can be analytically evaluated through the computation of $\{\mathbb{E}\left[T_{\text{d},i}\right]\}$. In [24], it is shown that this upper bound is equal to

$$\text{UB}_{T_{\text{net}}} = \frac{\mu}{n} + \sum_{i=2}^{n^{\text{R}}} \mu \frac{n-i}{(n-i+1)^2}. \tag{2.22}$$

Similarly, we can derive a lower bound on the network lifetime. This bound, for a fixed number of sensors, is obtained when all sensors' deaths occur in the same cluster. In this way, for a fixed topology, the highest possible probability of decision error is obtained at each instant and, consequently, the corresponding network lifetime is the shortest possible. This bound can be expressed as

$$\text{LB}_{T_{\text{net}}} \triangleq \mathbb{E}\left[T | n_{\text{crit}} = n_{\text{crit}}^{\text{LB}}\right] = \frac{\mu}{n} + \sum_{i=2}^{n_{\text{crit}}^{\text{LB}}} \mu \frac{n-i}{(n-i+1)^2}. \tag{2.23}$$

Expression (2.23) for $\text{LB}_{T_{\text{net}}}$ is derived from (2.22) by replacing $n_{\text{crit}}^{\text{R}}$ with $n_{\text{crit}}^{\text{LB}}$, which is obtained through simulations, since it depends on the network evolution. The value of $\text{LB}_{T_{\text{net}}}$ is smaller than that of $\text{UB}_{T_{\text{net}}}$, since $n_{\text{crit}}^{\text{R}} > n_{\text{crit}}^{\text{LB}}$. As previously mentioned, we consider an initial topology with two big clusters. In fact, this scenario allows to obtain the lowest probability of decision error at each instant, because the network topology is less unbalanced than in scenarios with a higher number of clusters, e.g., 8. Therefore, evolution of the lower bound (2.23) in correspondence to a scenario with two clusters leads to the tightest possible lower bound with respect to a scenario with no reclustering.

Finally, one needs to evaluate the extra time required by the application of the reclustering procedure. We will refer to this quantity as T_{R}. Under the given assumptions and since the probability that reclustering has happened is equal to 1/2 (the derivation of this probability is summarized in [24]), T_{R} can be expressed as

$$T_{\text{R}} = (n_{\text{crit}}^{\text{R}} - 1) T_{\text{RECL}}$$

where T_{RECL} represents the time required by a single reclustering operation. The duration of this time interval cannot be a priori specified, since it depends on the dimensions of the OK, CHANGE, and ALERT messages, the data-rate, and other network parameters. It is reasonable to assume that the longer is the average sensor lifetime μ, the shorter should be (proportionally) T_{RECL}. In other words, one could assume $T_{\mathrm{RECL}} = c \cdot \mu$, where c is small if μ is large and vice versa. In general, c can be chosen to model accurately the situation of interest.

Finally, one can define a *time penalty* as the ratio between the time necessary for the application of the reclustering protocol and the total time, given by the sum of reclustering and "useful" times (i.e., the time spent for data transmission). It follows that:

$$P^{\mathrm{time}} = \frac{T_{\mathrm{R}}}{T + \mathbb{E}[T_{\mathrm{net}}]} = \frac{(n_{\mathrm{crit}} - 1)T_{\mathrm{RECL}}}{(n_{\mathrm{crit}}^{\mathrm{R}} - 1)T_{\mathrm{RECL}} + \frac{\mu}{n} + \sum_{i=2}^{n_{\mathrm{crit}}^{\mathrm{R}}} \mu \frac{n-i}{(n-i+1)^2}}. \tag{2.24}$$

After a few mathematical passages, from (2.24) one obtains

$$P^{\mathrm{time}} \gtrsim \frac{(n - k^* - 1)c}{(n - k^* - 1)c + \frac{1}{n} + \ln(n-2) - \ln(k^* - 1)} \tag{2.25}$$

where we have used the fact that $\sum_{i=1}^{m} 1/i \simeq \ln m + 0.577$ [25].

From (2.25) and owing to the fact that k^* is approximately constant, one can analytically show that

$$\lim_{n \to \infty} P^{\mathrm{time}} \simeq 1 \quad \forall c.$$

In other words, if the number of sensors is large, for a fixed value of c the proposed reclustering algorithm does not guarantee a limited time penalty. Similarly, one can show that

$$\lim_{c \to 0} P^{\mathrm{time}} \simeq 0 \quad \forall n.$$

In other words, for a fixed number of nodes the reclustering protocol is effective, using the algorithm proposed in Sect. 2.2.2, *provided that* the duration of a single reclustering operation is sufficiently short (e.g., very small control packets are used).

2.2.3 Numerical Results

In Fig. 2.15, numerical results based on the application of the analytical framework derived in Sects. 2.2.2.1 and 2.2.2.2 are shown. In particular, (a) the average network lifetime $\mathbb{E}[T_{\mathrm{net}}]$ and (b) the critical number of deaths n_{crit} are shown as functions of the number of sensors n. The average network lifetime in a scenario with no reclustering (for various numbers of clusters) is compared with the upper and lower bounds derived in Sect. 2.2.2.2. The QoS condition is associated with $P_{\mathrm{e}}^* = 10^{-3}$

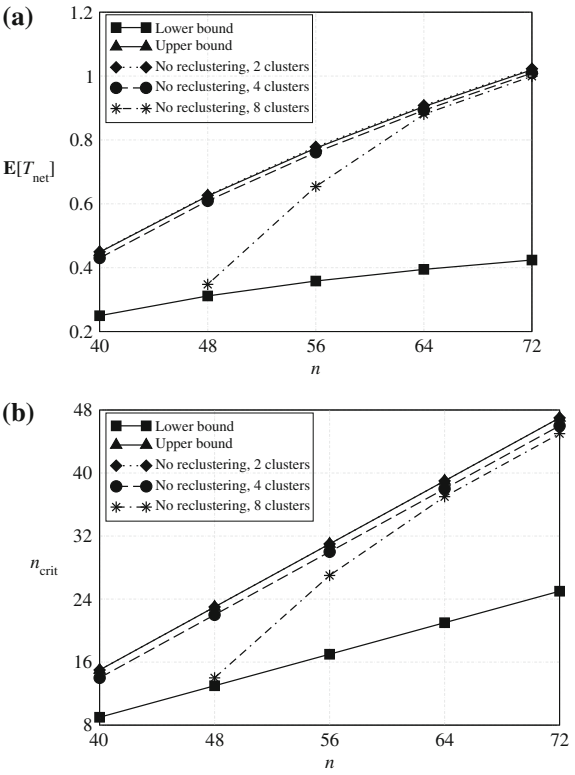

Fig. 2.15 Sensor network performance using the proposed reclustering algorithm: **a** network lifetime and **b** critical number of deaths, as functions of the number of sensors. The performance in the absence of reclustering (with 2, 4, and 8 clusters, respectively) is compared with the proposed upper bound $\mathrm{UB}_{T_{\mathrm{net}}}$ and lower bound $\mathrm{LB}_{T_{\mathrm{net}}}$. The QoS condition is $P_{\mathrm{e}}^{*} = 10^{-3}$ and the sensor SNR is set to 5 dB. The average sensor lifetime is $\mu = 1$

and the sensor SNR is set to 5 dB. In order to compare these results with those in Sect. 2.2.1.2, the distribution of the sensors' lifetime is assumed to be exponential with $\mu = 1$ aU. From the results in Fig. 2.15a, one can observe that, when the number of sensors increases, also the network lifetime becomes longer, since a larger number of sensors' deaths have to occur in order to violate the QoS condition. This is confirmed in Fig. 2.15b, where the critical number of sensors' deaths is shown as a function of the number of sensors. Moreover, as expected, the sensor network lifetime in the absence of reclustering is shorter than in the presence of ideal reclustering (with the proposed reclustering protocol), since the network topology becomes less and less uniform and, therefore, the probability of decision error becomes higher and higher. As previously shown in Fig. 2.13, when the initial number of clusters is equal to two, the network lifetime with no reclustering is very close to that corresponding to the application of the reclustering protocol. This is due to the fact that the sensors' deaths are, on average, equally distributed among the two clusters, i.e., there is a sort of "natural" reclustering. Finally, one can observe that when the number of clusters in the initial topology increases (e.g., is equal to 8) the network lifetime drastically reduces for *small* values of the number of sensors, since it is more difficult to satisfy the QoS condition. However, it is interesting to observe that for sufficiently large values of n, the lifetime penalty incurred by the presence of

a large number of clusters is negligible, suggesting that there may exist a minimum cluster dimension which guarantees acceptable performance. This is probably due to the fact that when the number of sensors is sufficiently large, the cluster dimension is also sufficiently large and, consequently, its lifetime is longer. Therefore, the lifetime of the entire sensor network is longer, since the network topology is less unbalanced.

2.2.4 Energy Budget

The analysis of the reclustering cost provided in Sect. 2.2.2 is ideal, since it does not consider the energy spent by the nodes in the network. Although this assumption is reasonable for the FCs and the AP,[4] this is not realistic for remote nodes (sensors) which need to rely on batteries with limited energy. Moreover, there is a delay associated with a packet transmission. In this subsection, the realistic network energy consumption is evaluated in the presence of ideal reclustering, using the reclustering protocol proposed in Sect. 2.2.2. In order to analyze this energy consumption, we will refer to a commercial WSN with a communication protocol based on the IEEE 802.15.4 standard (also considered in Sect. 2.2.6) [26]. In particular, while the first analysis does not take into account the energy of the sensor battery, we then show the impact of a limited battery energy at the sensors.

2.2.4.1 Analysis with Infinite Energy Battery at the Sensors

The energetic cost, for a single sensor, of the application of our reclustering algorithm can be written as

$$C_{\text{tot}}^{\text{en}} = P_{\text{t}}\, C_{\text{tot}}^{\text{time}} \tag{2.26}$$

where $C_{\text{tot}}^{\text{en}}$ is the total cost in terms of energy spent by a sensor, P_{t} is the transmit power at each sensor, and $C_{\text{tot}}^{\text{time}}$ is the total time cost associated with packet transmission. After a few manipulations, the total energetic cost can be written as [24]

$$C_{\text{tot}}^{\text{en}} = P_{\text{t}} \underbrace{\left\{ \frac{1}{2}\left\lceil \frac{L_{\text{cont}} + L_{\text{data}}}{R_{\text{b}}} \right\rceil \left(n_{\text{crit}}^{\text{R}} - 1\right) \right.}_{\substack{\text{Costfortransmissionof} \\ \text{controlpackets} : C_{\text{R}}^{\text{time}}}} + \underbrace{\left. \frac{L_{\text{data}}}{R_{\text{b}}} f_{\text{obs}} \sum_{i=1}^{n_{\text{crit}}^{\text{R}}} \mathbb{E}\left[\mathbb{T}_{\text{d},\beth}\right] \right\}}_{\substack{\text{Costfortransmission} \\ \text{ofdatapackets} : C_{\text{data}}^{\text{time}}}} \tag{2.27}$$

[4] In fact, they may be placed by the network designer so that they can be power-supplied.

where R_b is the data-rate [dimension: (bit/s)], L_{cont} and L_{data} are, respectively, the length of a control packet and data packet [dimension: (b/pck)], and f_{obs} is the observation frequency. Expression (2.27) for the energetic cost represents the total energy spent by any of the $n - n_{crit}^{R}$ surviving sensors after the network death. Obviously, this energetic cost represents a worst case, since there are n_{crit}^{R} nodes (i.e., those which die while the network is still alive) which spend a smaller amount of energy in their shorter lifetimes. An average cost per sensor can be easily computed using the same approach proposed above. In [24], the following expression for the average energy cost is derived:

$$\begin{aligned}\overline{C}_{tot}^{en} &= P_t(\overline{C}_R^{time} + \overline{C}_{data}^{time}) \\ &= P_t\left\{\frac{(n_{crit}^{R}-1)(L_{data}+L_{cont})}{4R_b} + \frac{L_{data}f_{obs}}{R_b n}\sum_{i=1}^{n_{crit}^{R}}\left((n-n^{R})\mathbb{E}\left[T_{d,i}\right] + \sum_{j=1}^{i}\mathbb{E}\left[T_{d,j}\right]\right)\right\}.\end{aligned} \tag{2.28}$$

Similarly to (2.24), we define the following *energy penalties*:

$$P^{en-1} \triangleq \frac{C_R^{en}}{C_{tot}^{en}} = \frac{C_R^{time}}{C_R^{time} + C_{data}^{time}} \tag{2.29}$$

$$P^{en-2} \triangleq \frac{\overline{C}_R^{en}}{\overline{C}_{tot}^{en}} = \frac{\overline{C}_R^{time}}{\overline{C}_R^{time} + \overline{C}_{data}^{time}} \tag{2.30}$$

where P^{en-1} is the *worst-case* penalty (associated with a sensor which survives until the end) and P^{en-2} is the *average-case* penalty (associated with the average energetic costs among all sensors in the network). As mentioned before, the energy penalties (2.29) and (2.30) take into account, with respect to (2.24), realistic network parameters, such as L_{data}, f_{obs}, R_b, and P_t.

In Fig. 2.16, the energy penalty is shown, as a function of the number of sensors n and the observation frequency f_{obs}, in the two cases previously highlighted: (a) *worst-case* energy consumption (obtained by using expression (2.29)) and (b) *average-case* energy consumption (obtained by using expression (2.30)). In order to compare the results in Fig. 2.16 with the results given in the previous subsections, we have set $P_e^* = 10^{-3}$ and $SNR_{sensor} = 5$ dB. Realistic values for the network parameters, provided by the IEEE 802.15.4 standard, correspond to $P_t = 1$ mW, $R_b = 250$ Kbit/s, $L_{data} = 1024$ bit/pck, and $L_{cont} = 80$ bit/pck.[5] One can note that for small values of the observation frequency (*rare observations*), the performance worsens since the network spends more time in reclustering than in

[5] In our analysis, we use the maximum possible data-rate allowed by the IEEE 802.15.4 standard, i.e., $R_b = 250$ Kbit/s. However, our experimental results show that only a maximum value $R_b = 25$ Kbit/s can be achieved by practical sensor networks [27]. Moreover, the length of data packets is the maximum allowed by the standard.

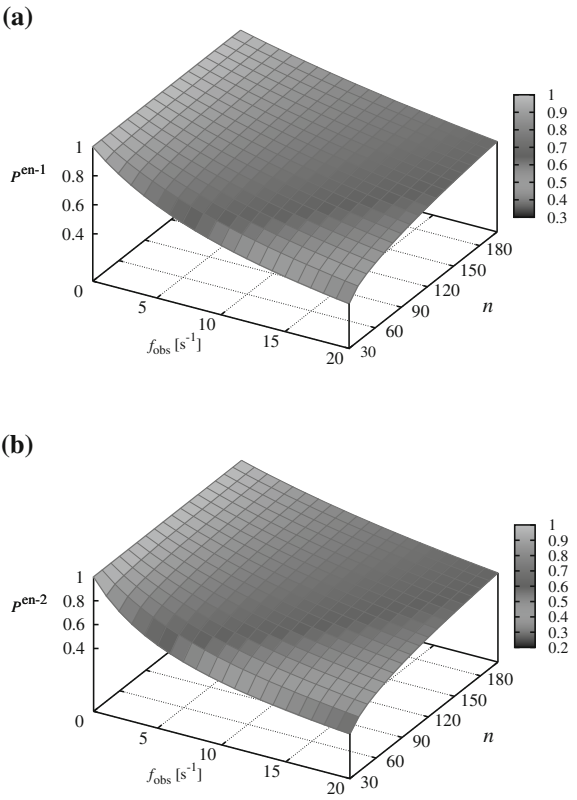

Fig. 2.16 Energy penalty, associated with the reclustering protocol, as a function of both the observation frequency f_{obs} and the number of sensors n. Two possible cases are considered: **a** *maximum* penalty (associated with a sensor which survives until the end) and **b** *average* penalty (among all the sensors in the network)

transmitting useful data. For a fixed value of the number of sensors n, the following limits hold:

$$\lim_{f_{obs}\to 0} P^{en-1} = \frac{C_R^{en}}{C_R^{en}} = 1 \quad \lim_{f_{obs}\to 0} P^{en-2} = \frac{\overline{C}_R^{en}}{\overline{C}_R^{en}} = 1.$$

Besides, one can observe that for increasing values of the observation frequency (*frequent observations*), the performance is better. In fact, for a fixed number of sensors, there is a larger number of data transmissions from the sensors to the AP and the value of D_R^{en} becomes increasingly negligible with respect to the value of D_{data}^{en}. Analytically, one can write

$$\lim_{f_{obs}\to \infty} P^{en-1} = \frac{1}{C_{data}^{en}} = 0 \quad \lim_{f_{obs}\to \infty} P^{en-2} = \frac{1}{\overline{C}_{data}^{en}} = 0.$$

Note that a high value of the observation frequency might not be admissible. In fact, in Sect. 2.2.2 we have supposed that the inverse of the observation frequency is much smaller than the time necessary to complete a transmission to the AP and, eventually, the reclustering protocol (hypothesis (a) in Sect. 2.2.2).

2.2.4.2 Analysis with Energy-Limited Battery at the Sensors

In the previous derivations, the proposed framework and the presented results have used arbitrary time units. However, it is of interest to map these arbitrary time units into realistic units. In order to do so, we assume that a node is equipped with a limited-energy battery with initial energy E_{battery} [dimension: (J)]. When a sensor battery energy exhausts, the sensor dies and, consequently, the network is closer to breaking the QoS condition. The average sensor lifetime [dimension: (s)] can be expressed as

$$\mathbb{E}[T_{\text{sensor}}] = \frac{E_{\text{battery}}}{\overline{P}}$$

where $\overline{P}$ is the average power depleted at the node [dimension: (W)]. In a realistic wireless sensor network (e.g., IEEE 802.15.4 wireless sensor networks [26]), four *states* are admissible at the node: (1) *transmission*, (2) *reception*, (3) *idle*, and (4) *sleep*. In this case, the average power depleted at the node is given by

$$\overline{P} = \sum_{i=1}^{4} P_i p_i \tag{2.31}$$

where P_i and p_i $(i = 1, 2, 3, 4)$ are, respectively, the power consumption in the ith state and the probability that the sensor is in the ith state—note that $P_1 = P_{\text{t}}$. Typically, in a IEEE 802.15.4 wireless sensor network $P_4 \ll 1$ and $p_2 \ll p_3, p_1$ [28]. Therefore, the average depleted power in (2.31) can be written as

$$\overline{P} \simeq P_1 p_1 + P_2 p_2$$

where $p_2 = 1 - p_1$ and $P_1 = P_2 = P_{\text{t}}$ [28]. Therefore, the average consumed power in (2.31) becomes

$$\overline{P} = P_{\text{t}}$$

and it follows that

$$\mathbb{E}[T_{\text{sensor}}] = \frac{E_{\text{battery}}}{P_{\text{t}}}. \tag{2.32}$$

Using the value of $\mathbb{E}[T_{\text{sensor}}]$ given in (2.32) for the computation of $C_{\text{tot}}^{\text{time}}$ according to the framework derived in Sect. 2.2.4.1, the lifetime of a realistic IEEE 802.15.4 wireless sensor network, with the parameters used to derive the results in Fig. 2.16, can be obtained. The sensor network lifetime values, associated with different battery energies at the sensors (typical for practical applications), are summarized in Table 2.3. In particular, a scenario with $n = 64$ sensors, $P_{\text{t}} = 1$ mW, and $f_{\text{obs}} = 20\,\text{s}^{-1}$ is considered. One can observe that the theoretical results given in Sect. 2.2.3 are confirmed also in a more realistic IEEE 802.15.4 WSN. However, note that for $n = 64$ sensors the network lifetime in the ideal

Table 2.3 Sensor network lifetime for a realistic IEEE 802.15.4 wireless sensor network in a scenario with $n = 64$ sensors, $P_t = 1$ mW, and $f_{obs} = 20\,s^{-1}$. The IEEE 802.15.4 parameters are the same considered in Fig. 2.16. Different values of the battery energy at a sensor are considered

Battery energy $E_{battery}$ (kJ)	Average sensor lifetime $\mathbb{E}[T_{sensor}]$ (days)	Sensor network lifetime C_{tot}^{time} (days)
12.96 (400 mAh, 9 V)	150	196
19.44 (600 mAh, 9 V)	224	294
31.68	365	480
32.4 (1 Ah, 9 V)	375	491

scenario is shorter than $\mathbb{E}[T_{sensor}]$, whereas it is longer in a realistic scenario. This behavior is due to the fact that our theoretical framework does not consider the delay associated with packet transmissions, as considered, instead, in the performance analysis for an IEEE 802.15.4 network.

2.2.5 Noisy Communication Links

The analysis of the sensor network lifetime proposed in Sect. 2.2.2 is quite general and, in particular, no assumption has been made on the communication links. However, the results presented in Sect. 2.2.3 are obtained under the assumption of *ideal* communication links. In a scenario with noisy communication links, two main differences, with respect to a scenario with ideal communication links, can be observed:

- for a given value of the sensor SNR, the presence of noisy communication links leads to a performance loss (i.e., higher probability of decision error);
- a probability of decision error floor can be visualized for high values of the sensor SNR.

These differences between the scenarios with ideal communication links and those with noisy communication links imply that the network lifetime will be shorter, since the QoS condition will be satisfied for a shorter time. Moreover, the presence of a probability of decision error floor implies that, for a given value of the sensor SNR, the QoS condition might never be satisfied. These considerations suggest that the QoS condition and the operating sensor SNR, for a given value of the number of sensors n, have to be properly chosen.

In Fig. 2.17, the CDF of the network lifetime is shown, as a function of time,[6] in a scenario with $n = 64$ sensors, uniform clustering, and noisy communication links.

[6] We recall that the time is measured, here, in arbitrary units. For more realistic scenarios, see the considerations at the end of Sect. 2.2.4.

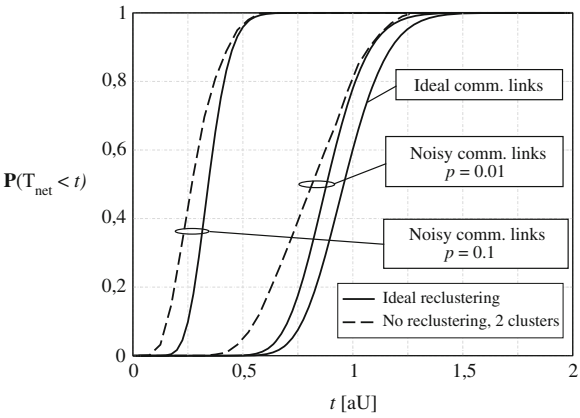

Fig. 2.17 CDF of the network lifetime, as a function of time, in a scenario with $n = 64$ sensors, uniform clustering, and noisy communication links. Two possible values for the cross-over probability are considered: (i) $p = 0.1$ and (ii) $p = 0.01$. The sensor SNR is set to 5 dB and the maximum tolerable probability of decision error is $P_e^* = 10^{-3}$

Two possible values for the cross-over probability are considered: (i) $p = 0.1$ and (ii) $p = 0.01$. For comparison, the curve associated with ideal communication links is also shown. The sensor SNR is set to 5 dB and the maximum tolerable probability of decision error is $P_e^* = 10^{-3}$. One can observe that the higher the noise intensity in the communication links is, the higher the CDF of the network lifetime becomes. In fact, in this case the transfer of information from the sensors to the AP is less reliable and, consequently, the probability of decision error becomes higher and higher and the QoS condition can be guaranteed for a shorter time. As in a scenario with ideal communication links, the presence of reclustering prolongs the network lifetime with respect to a scenario with no reclustering. Obviously, for a given reclustering strategy a scenario with ideal communication links corresponds to a longer network lifetime, since the probability of decision error is the lowest possible.

2.2.6 Throughput and Delay with Varying Sensor Network Lifetime

In this subsection, we evaluate the performance of a realistic IEEE 802.15.4 WSN subject to nodes' failures. In order to carry out this analysis, we resort, as in Sect. 2.1.5, to simulations using Opnet Modeler 11.5 [17] and a built-in model for IEEE 802.15.4 networks, provided by the NIST [18]. The network performance (in terms of number of transmitted packets, throughput, and delay) is analyzed in scenarios with no clustering (and, therefore, no reclustering). The goal of this subsection is to show the impact of different QoS conditions (given in terms of the required percentage of nodes' deaths which makes the network die) on different network performance indicators (e.g., throughput and delay). For the performance in the presence of relaying, the reader is referred to [29]. As discussed in Sect. 2.2.1, the performance of sensor networks with no clustering can be

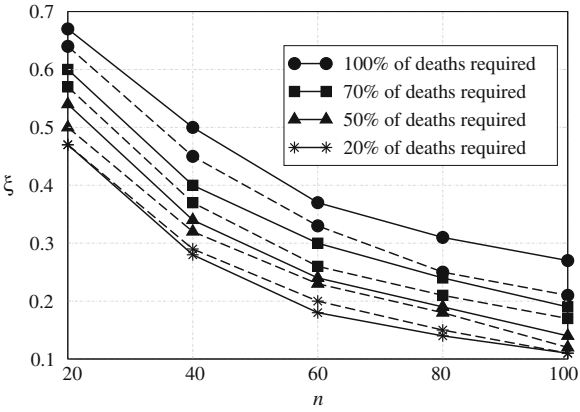

Fig. 2.18 Packet delivery fraction, as a function of the number of sensors n, in an IEEE 802.15.4 WSN with nodes' failures. Two possible distributions for a single sensor lifetime are considered: (**a**) exponential with $\mu = 300$ s (*solid lines*) and (**b**) uniform with $t_{\max} = 600$ s (*dashed lines*)

considered, from a network lifetime viewpoint, as a lower bound, since the probability of decision error is lower than in scenarios with clustering. In the simulations, the following parameters are considered: $R_b = 250$ Kbit/s, $L_{data} = 994$ bit/pck, and $g = 0.236$ s, where g is the packet interarrival time at the sensors. Moreover, no transmission of ACK packets is considered from the AP to the remote nodes. In all presented results, four QoS conditions will be considered: (i) network death corresponds to 100% of sensors' deaths (i.e., the network survives until there is a single sensor alive), (ii) network death corresponds to 70% of sensors' deaths, (iii) network death corresponds to 50% of sensors' deaths, and (iv) network death corresponds to 20% of sensors' deaths.

In Fig. 2.18, the packet delivery fraction is shown, as a function of the number of sensors n, for two possible distributions of a single sensor lifetime: (a) exponential with $\mu = 300$ s (solid lines) and (b) uniform with $t_{\max} = 600$ s (dashed lines). First, one can observe that the more stringent is the QoS condition, the lower is the throughput. In fact, a smaller number of transmissions is possible (since the network lifetime is shorter) and a larger number of collisions happens, because there is a large number of sensors that try to transmit to the AP and a larger number of packets is lost. Moreover, a scenario with uniform distribution of the sensors' lifetime has a lower throughput with respect to a scenario with exponential distribution, since more packets are lost due to the collisions.

In Fig. 2.19, the average MAC delay[7] D over all the received packets is shown, as a function of the number of sensors n, for two possible distributions of a single sensor lifetime: (a) exponential with $\mu = 300$ s (solid lines) and (b) uniform with $t_{\max} = 600$ s (dashed lines). Similarly to what happens to the throughput in Fig. 2.18, a larger number of collisions also causes a higher delay in receiving the packets. Therefore, scenarios with a uniform distribution of the sensors' lifetimes are characterized by a higher delay with respect to scenarios with an exponential

[7] The average MAC delay corresponds to the delay averaged over all packets which are correctly received at the MAC level during the Opnet simulations.

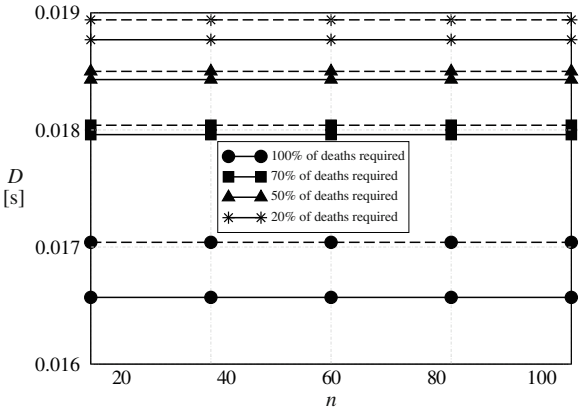

Fig. 2.19 Average MAC delay D, as a function of the number of sensors n, in an IEEE 802.15.4 WSN with nodes' failures. Two possible distributions for a single sensor lifetime are considered: **a** exponential with $\mu = 300$ s (*solid lines*) and **b** uniform with $t_{max} = 600$ s (*dashed lines*)

distribution. In this case as well, however, the more stringent is the QoS condition, the higher is the average MAC delay. Finally, the average MAC delay does not depend on the number of sensors, for a fixed QoS condition, since the number of surviving sensors is (almost) the same and, therefore, the average delay in the packet transmissions is constant.

2.3 Impact of Different SNRs at the Sensors

Consider now a generic scenario with different SNRs at the sensors. For the sake of simplicity, we consider a scenario with no clustering, i.e., direct communications between the sensors and the AP. In this case, a decision based on the majority-like fusion rule might not be the best choice. In fact, if a sensor is very noisy (i.e., its observation SNR is very small), its decision should be taken into account with a low level of reliability in the fusion process at the AP. Therefore, it would be reasonable to assign each sensor a weight proportional to its own SNR—this approach is similar to that proposed in [7], where the weights are assigned according to the link qualities. The AP could then make a final decision taking into account the weights assigned to the sensors. Note that the improvement, in terms of probability of decision error, comes at the price of a non-optimal network energy efficiency, since all sensors, even those with low SNR, have to send their decisions to the AP and waste the same amount of energy.

In the following, we consider a system where the AP takes into account the n local sensor decisions with the same weight, i.e., without considering their SNRs, and adopts a majority-like decision rule. In order to take into consideration the sensor SNR profile, the threshold for local decision at each sensor is properly optimized, as explained in detail in Sect. 2.3.1.2.

We now derive analytical expressions for the probability of decision error, distinguishing between a scenario with *ideal* communication links and a scenario with *noisy* communication links. In [30], the reader might found an analytical expression for the probability of decision error also in the case when no quantization is carried out at the sensors, i.e., when sensors transmit their local likelihood values.

2.3.1 Ideal Communication Links

2.3.1.1 Probability of Decision Error

Consider the first conditional probability at the right-hand side of (2.5) and define the threshold value k in the majority-like decision rule. There is an error, i.e., $\widehat{H} = H_1$ given that $H = H_0$, if $i \geq k$ sensors decide for H_1 when H_0 has happened. In this case, there can be $\binom{n}{i}$ combinations of sensors deciding for H_1. We denote as $\Omega_i(j)$ the jth possible combination ($j = 1, \ldots, \binom{n}{i}$) in a scenario where i sensors are in error.[8] Therefore, the conditional probability of interest can be expressed as follows:

$$\mathbb{P}\{\widehat{H} = H_1|H_0\} = \sum_{i=k}^{n} \sum_{j=1}^{\binom{n}{i}} \left\{ \prod_{\ell=1}^{i} \mathbb{P}\left\{u_\ell^{(\Omega_i(j))} = H_1|H_0\right\} \prod_{m=i+1}^{n} P\left(u_m^{(\Omega_i(j))} = H_0|H_0\right\} \right\} \tag{2.33}$$

where $\mathbb{P}\{u_\ell^{(\Omega_i(j))} = H_1|H_0\}$ is the probability that at the ℓth sensor, in the $\Omega_i(j)$th combination (out of the $\binom{n}{i}$ possible ones), a wrong decision is made when H_0 has happened.

Similarly, the second conditional probability at the right-hand side of (2.5) can be expressed as

$$\mathbb{P}\{\widehat{H} = H_0|H_1\} = \sum_{i=0}^{k-1} \sum_{j=1}^{\binom{n}{i}} \left\{ \prod_{\ell=1}^{i} \mathbb{P}\{u_\ell^{(\Omega_i(j))} = H_1|H_1\} \prod_{m=i+1}^{n} \mathbb{P}\{u_m^{(\Omega_i(j))} = H_0|H_1\} \right\} \tag{2.34}$$

[8] Note that $\Omega_i(j)$ depends also on n. However, for the sake of notational simplicity, this dependence is not explicitly indicated. The context should eliminate any ambiguity.

where $\mathbb{P}\{u_\ell^{(\Omega_i(j))} = H_1|H_1\}$ is the probability that at the ℓth sensor, in the $\Omega_i(j)$th combination, a correct decision is made when H_1 has happened.

2.3.1.2 Decision Threshold Selection at the Sensors

In the literature, it is shown that using the same threshold at every sensor is an asymptotically optimal solution *if and only if* the SNR at the sensors is constant [31]. In the currently considered scenario (with different SNRs at the sensors), it is not reasonable to use the same threshold at all sensors. Therefore, one needs to choose another criterion for local decisions at the sensors.

In this subsection, we consider a *locally optimal* decision scheme.[9] In other words, each sensor makes a binary decision which minimizes, for the corresponding SNR, its probability of (local) error—this corresponds to a *Person-By-Person Optimization (PBPO)* approach to distributed detection [32]. The optimal value for the threshold τ_i is such that

$$p(\tau_i|H_1)\mathbb{P}\{H_1\} = p(\tau_i|H_0)\mathbb{P}\{H_0\}. \tag{2.35}$$

In general, the computation of the probability of decision error, based on the evaluation of (2.33) and (2.34), depends on (i) the chosen value for k, (ii) the sequence of the detected phenomenon amplitudes $\{s_i\}$ at the sensors, (iii) the sequence of noise variances $\{\sigma_i\}$, and (iv) the sequence of thresholds $\{\tau_i\}$. Recalling the Gaussian model for the observable in (2.1), one can obtain [30]

$$\begin{aligned}\mathbb{P}\{u_\ell = H_1|H\} &= 1 - Q\left(\frac{\tau_\ell - s_\ell \cdot H}{\sigma_\ell}\right) \\ &= 1 - Q\left(\frac{1}{2}\sqrt{\mathrm{SNR}_{\mathrm{sensor}}^{(\ell)}} + \frac{1}{\sqrt{\mathrm{SNR}_{\mathrm{sensor}}^{(\ell)}}}\ln\frac{p_0}{1-p_0} - \sqrt{\mathrm{SNR}_{\mathrm{sensor}}^{(\ell)}}H\right).\end{aligned}$$

As expected, the probability of decision error does not depend on the sequences $\{s_i\}$ and $\{\sigma_i\}$ separately but, rather, only on the sequence of ratios $\{s_i/\sigma_i\}$, i.e., on the sequence of sensor SNRs. In other words, the probability of decision error depends on the sensor *SNR profile* $\{\mathrm{SNR}_{\mathrm{sensor}}^{(i)}\}$. Therefore, evaluating the system performance of the sensor network as a function of the sensor SNR profile is a meaningful problem.

2.3.2 Noisy Communication Links

Let us denote by p the cross-over probability of the BSCs (the same for all noisy communication links). In this case, the decision made at the ℓth sensor, i.e., u_ℓ,

[9] We are implicitly assuming that each sensor estimates its own observation SNR.

might be "flipped," with probability p, by the communication link. In particular, the component conditional probabilities in (2.5) depend on p. For instance, the conditional probability (2.33) has to be modified by replacing the decisions made locally by the sensors with the corresponding *received* decisions:

$$\mathbb{P}\{\widehat{H} = H_1|H_0\} = \sum_{i=k}^{n} \sum_{j=1}^{\binom{n}{i}} \left\{ \prod_{\ell=1}^{i} \mathbb{P}\{u_\ell^{(\Omega_i(j))-\text{rec}} = H_1|H_0\} \prod_{m=i+1}^{n} \mathbb{P}\{u_m^{(\Omega_i(j))-\text{rec}} = H_0|H_0\} \right\} \tag{2.36}$$

where $u_\ell^{(\Omega_i(j))-\text{rec}}$ and $u_m^{(\Omega_i(j))-\text{rec}}$ are the received versions of the local decisions $u_\ell^{(\Omega_i(j))}$ and $u_m^{(\Omega_i(j))}$, respectively. The conditional probability (2.34) has to be modified similarly. A generic term in (2.36) can then be expressed as follows:

$$\mathbb{P}\{u_\ell^{\text{rec}} = H_1|H_0\} = (1-p)Q\left(\frac{\tau_l}{\sigma_l}\right) + p\left[1 - Q\left(\frac{\tau_l}{\sigma_l}\right)\right]. \tag{2.37}$$

Since we are considering locally optimal selection of the decision thresholds at the sensors, there is no difference (in terms of the decision strategy at the sensors) between a scenario with ideal communication links and a scenario with noisy communication links. Therefore, the derivation considered in Sect. 2.3.1.2 for sensor threshold selection holds in this case as well.

2.3.3 Sensor SNR Profiles

As observed in Sect. 2.3.1.2, the probability of decision error ultimately depends on the *sensor SNR profile* $\{\text{SNR}_{\text{sensor}}^{(i)}\}$. A generic example of sensor SNR profile is shown in Fig. 2.20a: the sensor SNRs are generally not monotonically ordered. However, since it is always possible to reorder the sensor SNRs from highest to lowest, as shown in Fig. 2.20b, without loss of generality, one can restrict his/her attention to a scenario where the sensor SNR profile is *non-increasing*.

Based on the observation in the previous subsection, in order to characterize non-increasing sensor SNR profiles we consider four possible cases (the SNRs are expressed in dB):

$$\begin{aligned} &\text{Linear profile:} && \text{SNR}_i = \text{SNR}_0 - c \cdot i \\ &\text{Quadratic profile:} && \text{SNR}_i = \text{SNR}_0 - c \cdot i^2 \\ &\text{Cubic profile:} && \text{SNR}_i = \text{SNR}_0 - c \cdot i^3 \\ &\text{Hyperbolic profile:} && \text{SNR}_i = \frac{\text{SNR}_0}{1 + c \cdot i} \end{aligned} \tag{2.38}$$

where: $i = 0, \ldots, n-1$; n is the number of sensors; SNR_0 is the highest sensor SNR; and c is a suitable constant which uniquely characterizes the sensor SNR

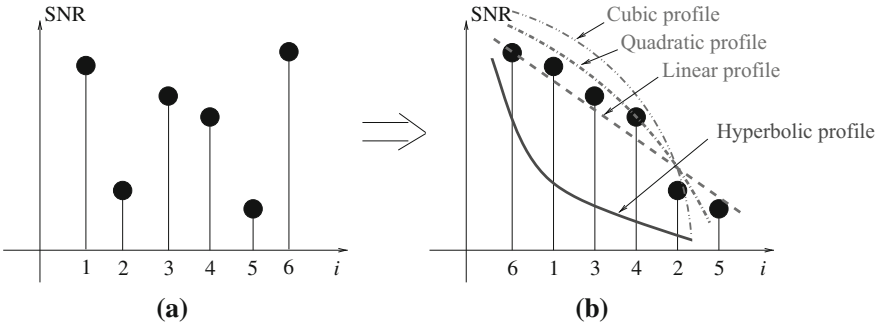

Fig. 2.20 Illustrative sensor SNR profile: **a** realistic and **b** reordered with non-increasing values of the SNRs. In particular, in (**b**) four possible interpolating profiles (linear, quadratic, cubic, and hyperbolic) are shown

profile *slope*. For this reason, we denote c as *slope coefficient*. A large value of c corresponds to a scenario where the sensor SNRs decrease rapidly (i.e., the corresponding realistic non-ordered sensor SNR profile is highly varying), whereas a small value of c corresponds to a scenario where the sensor SNRs are similar (i.e., the corresponding realistic non-ordered sensor SNR profile is almost constant). If $c = 0$, all profiles degenerate into a constant profile, i.e., $\mathrm{SNR}_i = \mathrm{SNR}_0$, $\forall i$. In Fig. 2.20b, illustrative graphical examples of the four profiles are shown. In the following, we will restrict our attention to scenarios with convex SNR profiles (linear, quadratic, and cubic), since concave profiles (e.g., hyperbolic) can be shown to lead to worse performance [30]. As one can see, by suitably setting the values of SNR_0 and c, a large number of realistic sensor SNR profiles can be characterized. This underlines the applicability of our framework. In Sect. 2.3.5, we will propose a simple experiment to characterize a realistic sensor SNR profile.

In (2.38), we have assumed that the maximum SNR and the slope coefficient c are the same for all profiles. However, in this case the winning profile is always the linear, since the sensor SNR at any position is higher than the corresponding one in any other profile. In order to obtain a "fair" comparison between the various profiles, one can impose that all the SNR profiles have the same average value, denoted as $\overline{\mathrm{SNR}}$.

- By imposing that the slope coefficient c is the same for all profiles, after a few manipulations one obtains that the maximum SNRs in the various cases need to be set as follows:

$$\begin{aligned}
\mathrm{SNR}_{0,\mathrm{l}} &= \overline{\mathrm{SNR}} + c\frac{n-1}{2} \\
\mathrm{SNR}_{0,\mathrm{q}} &= \overline{\mathrm{SNR}} + c\frac{(n-1)(2n-1)}{6} \\
\mathrm{SNR}_{0,\mathrm{c}} &= \overline{\mathrm{SNR}} + c\frac{n(n-1)^2}{4}.
\end{aligned} \tag{2.39}$$

• Specularly, imposing that the maximum SNR is the same for all the sensors, the slope coefficient in the four considered cases need to be set in the following way:

$$\begin{aligned} c_{\mathrm{l}} &= (\mathrm{SNR}_0 - \overline{\mathrm{SNR}})\frac{2}{n-1} \\ c_{\mathrm{q}} &= (\mathrm{SNR}_0 - \overline{\mathrm{SNR}})\frac{6}{(n-1)(2n-1)} \\ c_{\mathrm{c}} &= (\mathrm{SNR}_0 - \overline{\mathrm{SNR}})\frac{4}{n(n-1)^2}. \end{aligned} \tag{2.40}$$

Finally, one should observe that in (2.40) it must hold that $\mathrm{SNR}_0 - \overline{\mathrm{SNR}} \geq 0$.

We point out that throughout this subsection we make the implicit assumption that the SNR profiles are perfectly known and available at the AP. This is expedient for performance analysis. However, in a realistic scenario, the mechanisms to collect SNR values from the resource-constrained sensors may not be very accurate, and relying too much on them may not be helpful. Collecting the values accurately is a challenging problem, which needs further investigation. For example, the SNR values could be collected during a *training phase*, when each sensor computes its local SNR and send it to the AP. In Sect. 2.3.5, we propose a simple experimental validation of our theoretical assumptions.

2.3.4 Numerical Results

2.3.4.1 Ideal Communication Links

Let us first consider a sensor network with ideal communication links from the sensors to the AP. Moreover, the a priori probabilities of the phenomenon are such that $\mathbb{P}\{H_0\} = 10\mathbb{P}\{H_1\}$: this is meaningful for situations where a phenomenon is rare (e.g., the phenomenon under observation is an unusually high humidity level).

The following question is meaningful: for a given value of SNR_0, what are the conditions under which the use of a limited number of sensors (lower, for instance, than n) is the winning strategy? In order to answer this question, in Fig. 2.21 the probability of decision error is shown, as a function of the coefficient c, in a scenario with linear SNR profile. The lines correspond to analytical results, whereas the symbols are associated with Monte Carlo simulation results. Two possible values for the highest sensor SNR, i.e., SNR_0, are considered: 12 and 16 dB, respectively. For each value of the sensor SNR, various numbers of sensors are considered. Obviously, the curves corresponding to scenarios with only $n = 1$ sensor are constant with respect to c. The impacts of the parameters c and SNR_0 can be characterized as follows.

- For *small* values of c, i.e., in a scenario with almost constant SNR profile, the best performance is obtained using *all sensors*, regardless of the value of SNR_0.

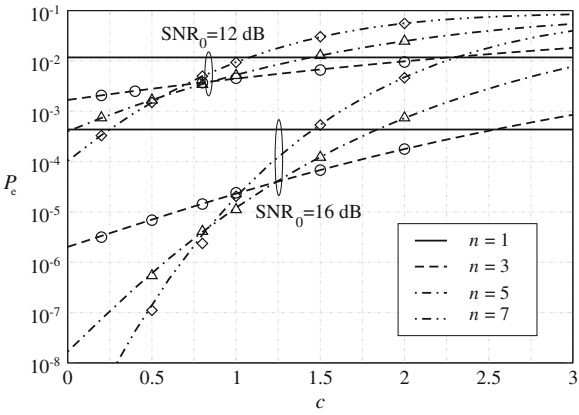

Fig. 2.21 Probability of decision error, as a function of the coefficient c, with SNR_0 equal to 12 and 16 dB, respectively. Various values of the number of sensors n are considered, in a scenario with *linear* sensor SNR profile. The *lines* correspond to analytical results, whereas the symbols are associated with simulation results

For *large* values of c (i.e., irregular sensor SNR profile before monotonic reordering), the best performance is obtained using only the sensors with *highest SNRs*. Note that the best asymptotic performance ($c \to \infty$) is obtained using only *the* sensor with highest SNR (SNR_0): however, the probability of decision error might be intolerably high.

- For low values of SNR_0, the impact of c is "mild," whereas for high values of SNR_0 the impact of c is relatively stronger. This behavior can be interpreted as follows. If *at least* one sensor is highly accurate, i.e., SNR_0 is high, then in order to optimize the network performance the right subset of sensors should be carefully chosen. In other words, the higher is the sensitivity of at least one sensor in observing the phenomenon, the more accurate the selection of a suitable subset of sensors has to be carried out.

As one can observe from Fig. 2.21, for a given value of c, the best performance is obtained selecting a specific number of sensors—those with highest SNRs, starting from the one with SNR_0. In order to characterize this behavior in more detail, in Fig. 2.22 the optimal value of the number of sensors to be selected is shown, as a function of c, for various values of SNR_0. The results in Fig. 2.22 show that (i) the optimal number of sensors is a decreasing function of c and (ii) the lower SNR_0 is, the faster the optimal number of sensors decreases for increasing values of c. A careful reader might wonder, at this point, why the optimal number of sensors does not reduce by one in correspondence with each vertical (decreasing) step. This behavior is due to the fact that the decision threshold τ_i at the ith sensor is computed according to (2.35), which represents a *locally optimal* threshold selection strategy. Therefore, one can conclude that such a threshold selection strategy is not *globally optimal* (from the entire distributed decision process), as observed in [33]. The individuation of globally optimal decision thresholds at the sensors in a scenario with non-constant sensor SNR profile goes beyond the scope of this book.

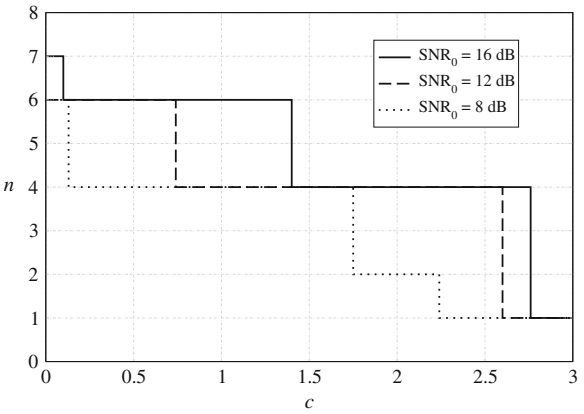

Fig. 2.22 "Optimal" number of sensors (for minimizing the probability of decision error), as a function of the coefficient c, in a scenario with *linear* sensor SNR profile and $\mathbb{P}\{H_0\} = 10\,\mathbb{P}\{H_1\}$. Three values for SNR_0 are considered

2.3.4.2 Noisy Communication Links

While in the previous section we have considered a scenario with *ideal* communication links, we now extend the previous analysis in order to evaluate the impact of the sensor SNR profile in the presence of noisy communication links. More precisely, in a simple network scenario with $n = 3$ sensors, we compare directly the performance with linear, quadratic, and cubic sensor SNR profiles. We do not consider the hyperbolic profile, since we have shown in Sect. 2.3.4.1 that the overall performance with this profile is worse than that with the other profiles—in fact, in the presence of a hyperbolic profile the average sensor SNR has to be very high in order to obtain an acceptable performance level. We evaluate the probability of decision error in a scenario with *all noisy* communication links (considering two values for the cross-over probability p, equal to 10^{-3} and 10^{-1}, respectively) and, for comparison, in a scenario with all ideal links.

In Fig. 2.23, the probability of decision error is shown, as a function of the slope coefficient c, in various scenarios with $\mathrm{SNR}_0 = 16$ dB and $\mathbb{P}\{H_0\} = 10\mathbb{P}\{H_1\}$.

In Fig. 2.24, the same sensor network scenario is considered, but the *average* sensor SNR is kept constant to $\overline{\mathrm{SNR}} = 16$ dB—for each value of c, the corresponding value of SNR_0 is determined according to (2.39). On the basis of the results shown in Figs. 2.23 and 2.24, it is possible to characterize, performance-wise, the interaction between the sensor SNR profile and the communication noise as follows.

- In a scenario with a *common* value of SNR_0, the impact of the sensor SNR profile is very similar in scenarios with ideal communication links and with noisy communication links. For the same value of c, the probability of decision error increases if the profile changes from linear to cubic. Obviously, for $c = 0$ the performance with the three profiles coincides. Moreover, asymptotically (for large values of c) the probability of decision error is the same regardless of the profile. Therefore, it is possible to identify a critical value of c beyond which the impact of the sensor SNR profile is the highest.

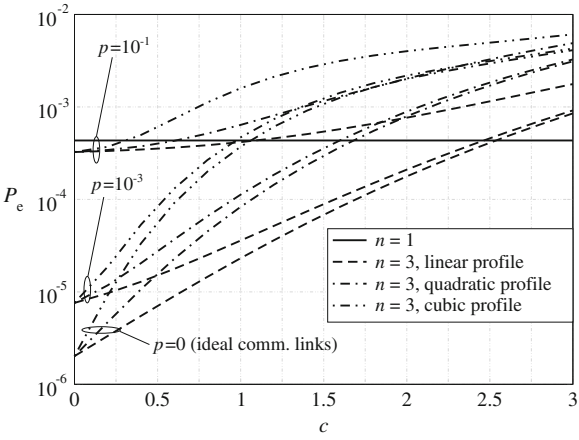

Fig. 2.23 Probability of decision error, as a function of the coefficient c, in a scenario with $n = 3$ sensors. The common value of the maximum sensor SNR is $\text{SNR}_0 = 16$ dB. Three possible scenarios are considered: (i) all ideal links ($p = 0$), and all noisy links with (ii) $p = 10^{-3}$ and (iii) $p = 10^{-1}$, respectively. For comparison, the performance with $n = 1$ sensor is also shown (*horizontal solid line*)

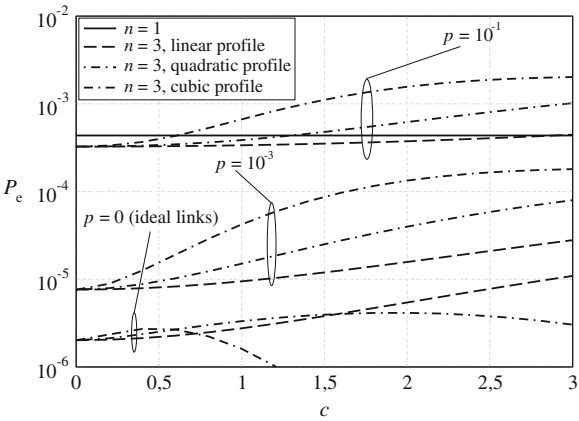

Fig. 2.24 Probability of decision error, as a function of the coefficient c, for the same scenario of Fig. 2.23 and a common *average* value of the sensor SNR equal to $\overline{\text{SNR}} = 16$ dB

The impact of the noise is strong for small values of c, whereas it becomes negligible for large values of c. In fact, for any given profile, the curves associated with ideal links and those associated with noisy links tend to coincide for increasing values of c. In other words, the less regular is the sensor SNR profile (i.e., the larger is c), the milder is the impact of the noise in the communication links. On the other hand, if the sensor SNR is very similar across the sensors, then the noise in the communication links has a severe impact of the network performance. This latter scenario is analyzed in detail in [3].

- In a scenario with a common value of $\overline{\text{SNR}}$, rather than a common maximum sensor SNR, the $P_e - c$ curves do not tend to coincide for large values of the slope coefficient c. In other words, the impact of the value of c in a scenario with common $\overline{\text{SNR}}$ is stronger than in a scenario with common SNR_0. On the other

hand, for small values of the slope coefficient c, the performance in a scenario with common $\overline{\text{SNR}}$ is similar to that in a scenario with common SNR_0.
From the results in Fig. 2.24, one can also make another observation. In the presence of ideal communication links, for increasing values of c the best performance is obtained by quadratic and cubic profiles. On the opposite, in the presence of noisy communication links, for increasing values of c the best performance is given by a linear sensor SNR profile.

2.3.5 Experimental Validation

In this subsection, we show experimental results relative to the SNRs measured at the sensors, in order to validate the theoretical models proposed in this section. In particular, we evaluate the Received Signal Strength Indication (RSSI) in order to obtain *sensor SNR-like* profiles. Equivalently to the RSSI, one could also use the *Path Loss* indicator. In fact, the following equation (in logarithmic scale) holds:

$$P_{\text{t}} = \text{RSSI} + \text{PathLoss}$$

where P_{t} is the transmit power [dimension: (dBm)] and Path Loss is the power reduction incurred by propagation [dimension: (dB)]. Since in our experiments we set $P_{\text{t}} = 0$ dBm, one easily obtains:

$$\text{RSSI} = -\text{PathLoss}.$$

The main idea of our experiments is the following. A mobile mote periodically sends a message, called *beacon*, whereas n remote nodes, at fixed positions with respect to the mobile mote, receive the beacon and store the received power. Finally, a vector of n power levels is obtained, and an SNR-like profile can be derived. The experimental set-up[10] is schematically shown in Fig. 2.25, from (a) practical and (b) logical viewpoints, respectively. We deploy four MicaZ nodes at the vertices of a square area of $90 \times 90\,\text{cm}^2$, and the remaining mobile (beacon) mote acts as the event "generator" and is denoted as firing mote (fm). As shown in Fig. 2.25, four nodes are placed at the vertices of the network surface. The fm moves inside the network, sending messages to the fixed nodes. Note that in the considered experimental set-up, the observed phenomenon corresponds to the message sent by the mobile node. In order to replicate the theoretical analysis,

[10] Since our experiments are developed in a laboratory environment, there is furniture all around the square area where the sensors are deployed. However, we can consider the reflected signals negligible.

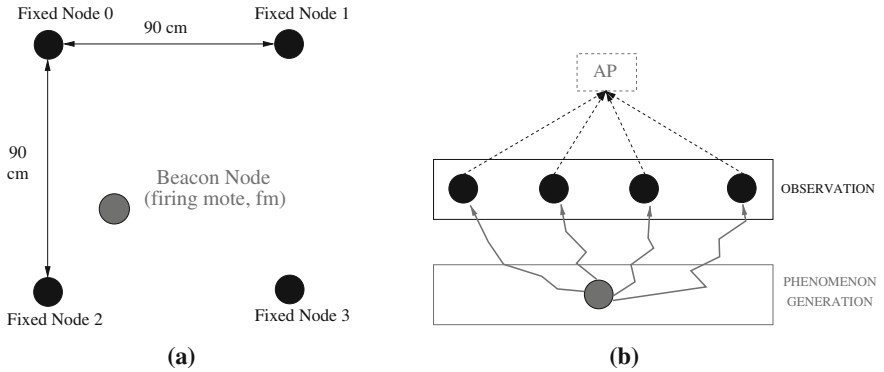

Fig. 2.25 Experimental set-up: **a** practical scheme with five motes (one "firing/beacon node" and four fixed nodes), deployed over a square network surface with area equal to $90 \times 90\,\text{cm}^2$, and **b** its corresponding logical scheme. The considered platforms are constituted by MicaZ motes using a communication protocol compliant with the IEEE 802.15.4 standard

after receiving the message from the fm, the four fixed nodes should take a decision (e.g., based on the received power), and send their decisions to an AP. Since our goal, in this subsection, is to characterize the sensor SNR profile, we do not consider the communication phase from the sensors to the AP.

Two experiments have been run:

- the fm, which sends the beacon, is very close to one of the remote (fixed) nodes;
- the fm is in the middle between the network center and one of the four vertices of the square network surface, i.e., a fixed node.

In Fig. 2.26, the Path Loss is shown, as a function of the remote node IDs (indicated in Fig. 2.25a), in two different scenarios: (a) the fm is very close to one of the fixed nodes, and (b) the fm is in the middle between the network center and one of the fixed nodes. As one can see from Fig. 2.26a, the lowest Path Loss is obtained, as expected, in correspondence to the nearest remote node. In this case, the profile described is a *heavyside-like* function, since only the fixed node closest to the fm senses a high RSSI (or, equivalently, a low Path Loss), while the others do the opposite. In Fig. 2.26b, the fm is in a more central region and, therefore, the measured power profile is, as expected, smoother than that observed in Fig. 2.26a.

Rearranging the values in Fig. 2.26b in an increasing order, one can obtain a decreasing profile, as described in the previous subsections, of Path Loss or RSSI measurements. In Fig. 2.27, the *Path Loss* profile is shown, as a function of the mote ID, for the four different cases (relative to the position of the mobile mote) considered in Fig. 2.26b. As one can observe, on the average, the profile is approximately linear.

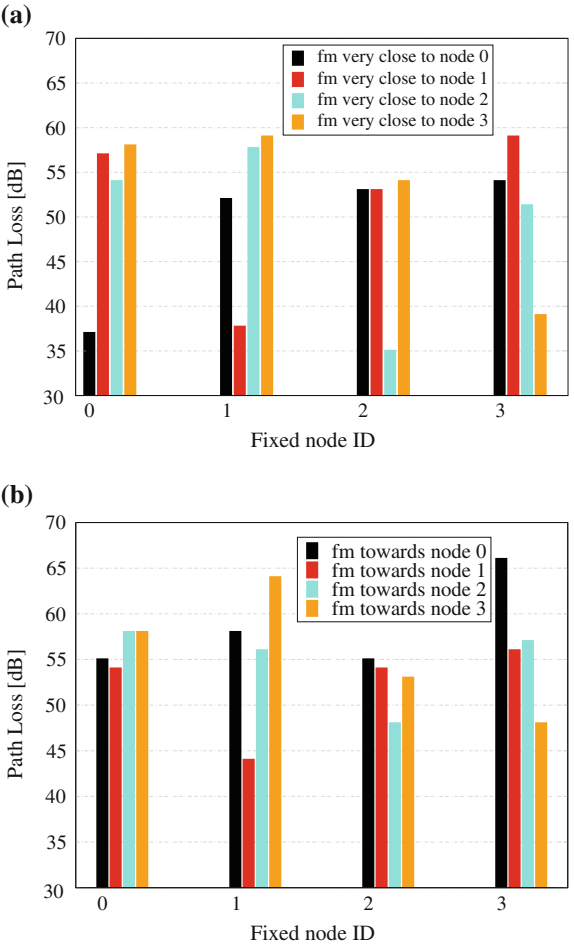

Fig. 2.26 Path Loss profiles in the presence of four MicaZ motes sensing a fm. The fm is placed either **a** very close to one of the vertices or **b** between the center of the area and one of the vertices

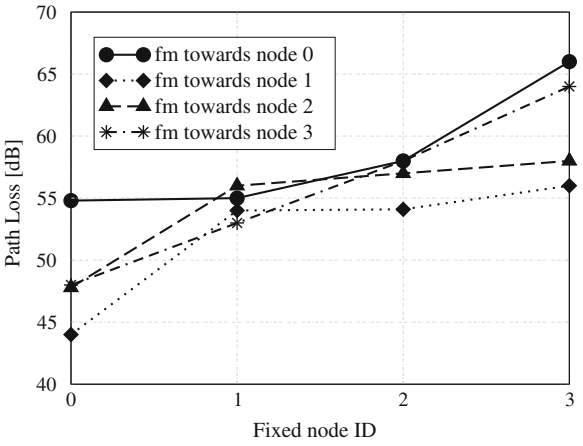

Fig. 2.27 Reordered Path Loss profiles in the scenarios considered in Fig. 2.26b

2.4 On the Interplay Between Decoding and Fusion

2.4.1 Distributed Channel Coding and Detection/Decoding/Fusion Strategies

In Fig. 2.28, a pictorial description of the considered sensor network model is shown. There are source nodes (the sensors), which observe (in a noisy manner) a spatially constant phenomenon and send their decisions to the AP, possibly using channel coding. The presence of a relay is also considered and a simple relaying strategy is proposed. The impact of multiple access interference is not investigated here: in other words, we assume orthogonal transmissions to the AP (e.g., perfect transmission scheduling between the sensors and, if present, the relay). The AP performs the following operations:

- *detection* of the observables, taking into account their statistical characterization;
- *decoding* of the embedded error correction code (when used);
- *fusion* of the decoded data to estimate the status of the phenomenon under observation.

Note that some of the elements in Fig. 2.28 are present only in specific scenarios—for instance, the relay node and the decoding block in the AP appear only in coded scenarios.

2.4.1.1 Repetition Coded Sensor Network

A sensor network with multiple observations (M consecutive and independent observations of the same phenomenon) can be interpreted as a system embedding a *repetition code* (with code rate $1/M$) at each sensor. In this case, redundant

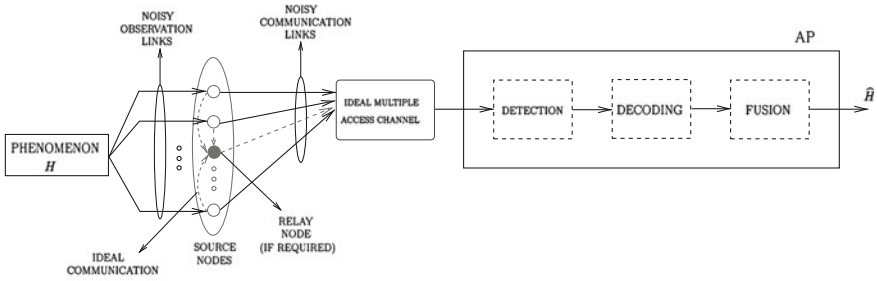

Fig. 2.28 Pictorial description of the considered sensor network schemes. *Solid lines* are associated with *mandatory* elements (either blocks or connections), whereas *dashed lines* are associated with *optional* elements

information is not sent by a relay, but from the sensors themselves through M consecutive transmission acts per sensor.

2.4.1.2 Systematic Block Coded Sensor Network

In order to embed a *systematic* block channel code into a sensor network, we propose a simple relaying strategy. More precisely, we assume that each sensor transmits its (uncoded) decision to the AP and, owing to the broadcast nature of the wireless medium, also to the relay. Upon reception of the decisions from the sources, the relay, by using a systematic block code, generates parity bits and sends them to the AP. For example, a $(n_{\text{cod}}, n) = (7, 4)$ systematic Hamming code [34, p. 562] can be embedded into a sensor network with $n = 4$ sensors and one relay, which generates $n_{\text{cod}} - n = 3$ bits according to the parity-check equations of the Hamming code. Assuming (as mentioned) that each sensor can reach both the AP and the relay in a single transmission act, the total number of transmission acts in the proposed sensor network is n_{cod}. The equivalent code rate of this distributed coded scheme is $R_{\text{c}} = n/n_{\text{cod}} = 4/7$. Note, however, that the connections between the sensors and the relay have to be *ideal* (i.e., with no communication noise) in order for the proposed schemes to be applicable. This assumption is reasonable provided that, for example, the relay is relatively closer to the sensors than the AP is. In Sect. 2.4.4, we will comment on the impact of the noise in the communication links from the sensors to the relay.

With a slight abuse of notation, in the following we will denote a scenario as "coded" only if a block channel code is embedded into the network structure, in order to distinguish it from a scenario with multiple observations (i.e., repetition coded).

2.4.1.3 Communication Schemes

In a coded scenario with Binary Phase Shift Keying (BPSK) and Rayleigh faded links, the observable at the output of the communication channel can be expressed as

$$r_i = f_i(2c_i - 1)\sqrt{E_{\text{c}}} + w_i \quad i = 1, \ldots, n_{\text{cod}} \tag{2.41}$$

where $c_i \in \{0, 1\}$ is the symbol transmitted from either a sensor (c_i is an information bit, $i = 1, \ldots, n$) or the relay (c_i is a parity bit, $i = n + 1, \ldots, n_{\text{cod}}$), $\{w_i\}$ are statistically independent AWGN samples with the same distribution $\mathcal{N}(0, N_0/2)$, N_0 being the single-sided noise power spectral density, $E_{\text{c}} \triangleq R_{\text{c}} E_{\text{b}}$ is the energy per coded bit, E_{b} being the energy per information bit, and f_i is a random variable with Rayleigh distribution—perfectly coherent demodulation is considered. Under the assumptions of independence between consecutive fading samples (e.g., through the use of channel interleaving) and that $\mathbb{E}[|f_i|^2] = 1$, the BER at the output of the detector at the AP is [35]

$$p^{\text{Rayleigh}} = \frac{1}{2}\left[1 - \sqrt{\frac{R_c\gamma_b}{1 + R_c\gamma_b}}\right] \tag{2.42}$$

$\gamma_b \triangleq E_b/N_0$ is the SNR at the AP. A scenario with AWGN communication links can be modeled using (2.41), by imposing $f_i = 1$ $(i = 1, \ldots, n_{\text{cod}})$. In this case, the BER at the output of the detector at the AP can be written as [35]

$$p^{\text{AWGN}} = Q\left(\sqrt{2R_c\gamma_b}\right). \tag{2.43}$$

In general, one can denote as p the BER at the output of the detector, where p has a specific expression (either (2.43) or (2.42)), depending on the communication channel and the detection strategy (this is also compliant with the initial approach proposed in Sect. 2.1). For simplicity, we assume that p is the same for all sensor-AP links.

In all above communication schemes, the probability of decision error at the AP can be evaluated by computing the conditional probabilities $\mathbb{P}\{\widehat{H} = H_i | H = H_j\}$ in (2.5) $(i, j = 0, 1, i \neq j)$. These values depend on the presence/absence of channel coding and on the detection/decoding/fusion strategy at the AP, as will be described in the following subsections, distinguishing on the basis of the observations at the sensors.

2.4.2 Ideal Observations at the Sensors

In order to obtain performance benchmarks, we first consider scenarios where the spatially constant phenomenon H is detected by the sensors ideally. In this case, we distinguish between AP structures where the decoding and fusion operations are either separate or joint.

2.4.2.1 Separate Decoding and Fusion

When the decoding and fusion operations are separate, assuming majority-like fusion the conditional probabilities at the right-hand side of (2.5) can be computed as follows:

$$\mathbb{P}\{\widehat{H} = H_1 | H = H_0\} = \sum_{i=k}^{n} \binom{n}{i} (p_{\text{ch}}^{\text{ideal}})^i (1 - p_{\text{ch}}^{\text{ideal}})^{n-i} \tag{2.44}$$

$$\mathbb{P}\{\widehat{H} = H_0 | H = H_1\} = \sum_{i=0}^{k-1} \binom{n}{i} (1 - p_{\text{ch}}^{\text{ideal}})^i (p_{\text{ch}}^{\text{ideal}})^{n-i} \tag{2.45}$$

where the repeated trials formula has been used [9], k (i.e., the majority decision threshold) is $\left\lfloor \frac{n}{2} \right\rfloor + 1$, and the probability $p_{\text{ch}}^{\text{ideal}}$ depends on the noisy

communication link model and the specific distributed channel coding strategy. Note that the upper index of the sum in (2.44) is n (and not n_{cod}) also in coded scenarios, since the information from the relay (i.e., the parity bits) is not used in the *fusion* process (only the systematic bits are used). The parity bits are used only in the *detection*/*decoding* process.

Since the local sensors' decisions are error-free, $p_{\text{ch}}^{\text{ideal}}$ and $1 - p_{\text{ch}}^{\text{ideal}}$ in (2.44) and (2.45) correspond to the probabilities of error and correct decision at the detector output, respectively. In an "uncoded scenario" (i.e., $n_{\text{cod}} = n$), it holds that $p_{\text{ch}}^{\text{ideal}} = p$. In a scenario with multiple observations, the AP preliminary decides for the phenomenon status at each sensor through a majority fusion rule over the M consecutive decisions sent by that sensor. In this case, $p_{\text{ch}}^{\text{ideal}}$ can be expressed, similarly to (2.44), as

$$p_{\text{ch}}^{\text{ideal}} = \sum_{i=k_{\text{NC}}}^{M} \binom{M}{i} p^i (1-p)^{M-i} \tag{2.46}$$

where $k_{\text{NC}} \triangleq \lfloor \frac{M}{2} \rfloor + 1$. In a coded scenario and for sufficiently small values of p, the following approximation holds [34]:

$$p_{\text{ch}}^{\text{ideal}} \simeq \binom{n_{\text{cod}} - 1}{t} p^{t+1}$$

where $t = (d_{\min} - 1)/2$ is the number of errors which can be corrected by a code with minimum distance $d_{\min}$ [34, 36]. We point out that, provided that $1/M = n/n_{\text{cod}}$, the comparison between coded schemes and schemes with multiple observations is consistent from an energetic viewpoint.

2.4.2.2 Joint Decoding and Fusion

In a scenario with multiple (M) independent observations at the sensors, joining the decoding and fusion operations consists in adopting a majority fusion rule over all the $n \times M$ bits sent from the sensors to the AP. In this case, the probability of decision error becomes

$$P_{\text{e}}^{\text{mult.obs.}} = \frac{1}{2} \left[\sum_{i=k_{\text{M}}}^{n \times M} \binom{n \times M}{i} p^i (1-p)^{n \times M - i} + \sum_{i=0}^{k_{\text{M}}-1} \binom{n \times M}{i} (1-p)^i p^{n \times M - i} \right] \tag{2.47}$$

where $k_{\text{M}} \triangleq \left\lfloor \frac{n \times M}{2} \right\rfloor + 1$ is the majority decision threshold.

In a coded scenario, the receiver with joint decoding and fusion can be designed as follows. Since the considered sensor networks embed *systematic* codes, we denote as $[u_1^{(j)}, \ldots, u_n^{(j)}, b_1^{(j)}, \ldots, b_{n_{\text{cod}}-n}^{(j)}]$ $(j = 0, 1)$ the entire sequence of bits transmitted by the sensors ($u_i^{(j)}$ from sensor i) and the relay ($\{b_i\}_{i=1}^{n_{\text{cod}}-n}$ from the

relay) in correspondence to the phenomenon status H_j. Note that in the current case with a spatially constant binary phenomenon and ideal observations at the sensors, $(u_1, \ldots, u_n)$ is either $(0, \ldots, 0)$ or $(1, \ldots, 1)$. In other words, in the presence of *ideal* observations, only two codewords, denoted as $\boldsymbol{c}^{(0)}$ and $\boldsymbol{c}^{(1)}$, are allowed—this does not hold with noisy observations, as will be shown in Sect. 2.4.3. In particular, $\boldsymbol{c}^{(0)} = (0, \ldots, 0)$. In all cases considered in this subsection, it will also hold that $\boldsymbol{c}^{(1)} = (1, \ldots, 1)$.

Given that decoding and fusion are joint, two possible detection strategies at the AP can be devised:

- hard-output detection is followed by (hard-input) joint decoding/fusion;
- detection, decoding, and fusion are all joined together.

In the former case, the Maximum A posteriori Probability (MAP) joint decoding/fusion strategy can be formalized as

$$\widehat{H} = \underset{j=0,1}{\operatorname{argmax}} \, \mathbb{P}\{\boldsymbol{c}^{(j)} | \boldsymbol{c}_{\mathrm{rx}}\} = \underset{j=0,1}{\operatorname{argmax}} \, \mathbb{P}\{\boldsymbol{c} | \boldsymbol{c}^{(j)}\} \mathbb{P}\{\boldsymbol{c}^{(j)}\} \tag{2.48}$$

where $\boldsymbol{c}_{\mathrm{rx}}$ is the codeword at the output of the detector at the AP. Since only two codewords $\boldsymbol{c}^{(0)}$ and $\boldsymbol{c}^{(1)}$ are used, the a priori probability of the sequence $\boldsymbol{c}^{(j)}$ is equal to the a priori probability of the phenomenon status H_j, i.e., $\mathbb{P}\{\boldsymbol{c}^{(j)}\} = p_j = 1/2$. Owing to the independence of the communication channels (conditionally on the transmitted bits), the MAP decoding/fusion strategy in (2.48) can be rewritten as

$$\widehat{H} = \underset{j=0,1}{\operatorname{argmax}} \, p_j \prod_{i=1}^{n_{\mathrm{cod}}} \mathbb{P}\{c_{i,\mathrm{rx}} | c_i^{(j)}\}. \tag{2.49}$$

After a few manipulations, the MAP decoding/fusion strategy in (2.49) can be finally formulated as

$$\left(\frac{1-p}{p}\right)^{2\vartheta(1,\boldsymbol{c}_{\mathrm{rx}})-n_{\mathrm{cod}}} \underset{H_1}{\overset{H_0}{\gtrless}} 1. \tag{2.50}$$

where $\vartheta(1, \boldsymbol{c}_{\mathrm{rx}})$ is the number of 0's in $\boldsymbol{c}_{\mathrm{rx}}$.

At this point, one can evaluate the probability of decision error in (2.5). In particular, the terms $\left\{\mathbb{P}\{\widehat{H} = H_i | H = H_j\}\right\}$ $(i, j = 0, 1, \ i \neq j)$ can be computed from the decision rule (2.50). After a few manipulations, one obtains:

$$P_{\mathrm{e}} = \frac{1}{2}\left[\sum_{k=k^*}^{n_{\mathrm{cod}}} \binom{n_{\mathrm{cod}}}{k} p^k (1-p)^{n_{\mathrm{cod}}-k} + \sum_{k=0}^{k^*-1} \binom{n_{\mathrm{cod}}}{k} (1-p)^k p^{n_{\mathrm{cod}}-k}\right]$$

where we have used the fact that $\vartheta(1, \boldsymbol{c}_{\mathrm{rx}})$ is a binomial random variable with parameters n_{cod} and p, $\boldsymbol{c}^{(1)} = \mathbf{1}$, and k^* is defined as follows:

$$k^* = \min\{1, \ldots, n_{\text{cod}}\}$$
$$\text{s.t.} \left(\frac{1-p}{p}\right)^{2k^*-n_{\text{cod}}} > 1.$$

In the case with joint detection/decoding/fusion, we first consider a scenario with Rayleigh faded links, and we denote by $\boldsymbol{f} = [f_1, \ldots, f_{n_{\text{cod}}}]$ the fading samples and by $\boldsymbol{r} = [r_1, \ldots, r_{n_{\text{cod}}}]$ the observables at the output of the communication links. Under the assumption of perfect channel state information at the AP, the MAP detection/decoding/fusion strategy can be formulated as[11] [36]

$$\widehat{H} = \underset{j=0,1}{\text{argmax}}\, p\left(\boldsymbol{r}|\boldsymbol{c}^{(j)}, \boldsymbol{f}\right)\mathbb{P}\{\boldsymbol{c}^{(j)}|\boldsymbol{f}\} = \underset{j=0,1}{\text{argmax}}\, p_j \prod_{i=1}^{n} p\left(r_i|c_i^{(j)}, f_i\right) \tag{2.51}$$

where we have used the facts that the observables are conditionally independent given $\{c_i^{(j)}\}$ and the coded bit $c_i^{(j)}$ is independent of the fading sample f_i. Discarding $p_j = 1/2$, from (2.51) one can derive, after a few manipulations, the following decision rule:

$$\sum_{i=1}^{n_{\text{cod}}} r_i f_i c_i^{(1)} \underset{H_0}{\overset{H_1}{\gtrless}} 0. \tag{2.52}$$

On the basis of (2.52) and recalling that a linear combination of Gaussian random variables is still a Gaussian random variable [9], after a few manipulations the probability of decision error at the AP (2.5) becomes

$$P_{\text{e}} = \frac{1}{2}\left[Q\left(2\frac{\sqrt{R_{\text{c}}E_{\text{b}}}\sum_{i=1}^{n_{\text{cod}}} f_i c_i^{(1)}}{\sqrt{N_0\sum_{i=1}^{n_{\text{cod}}} f_i^2 (c_i^{(1)})^2}}\right) + \Phi\left(-2\frac{\sqrt{R_{\text{c}}E_{\text{b}}}\sum_{i=1}^{n_{\text{cod}}} f_i (2c_i^{(1)} - 1)c_i^{(1)}}{\sqrt{N_0\sum_{i=1}^{n_{\text{cod}}} f_i^2 (c_i^{(1)})^2}}\right)\right] \tag{2.53}$$

where $\Phi(x) \triangleq 1 - Q(x)$. Observe that (2.53) depends on the particular sequence of fading samples $\{f_i\}$.

An expression for the probability of decision error in the case of AWGN links can be directly obtained from (2.53) by imposing $f_i = 1$ ($i = 1, \ldots, n_{\text{cod}}$). In particular, in the presence of a code with $\boldsymbol{c}^{(1)} = \mathbf{1}$ (recall that, in all cases, $\boldsymbol{c}^{(0)} = \mathbf{0}$) it can be shown that

$$P_{\text{e}} = Q\left(\sqrt{2n_{\text{cod}}R_{\text{c}}\gamma_{\text{b}}}\right) = Q\left(\sqrt{2n\gamma_{\text{b}}}\right).$$

[11] In (2.51) and in the remainder of this subsection, the uppercase $\mathbb{P}$ is used to denote the probability of an event, whereas the lowercase p is used to denote the conditional probability density function (p.d.f.) of a random variable.

2.4.3 Noisy Observations at the Sensors

We now extend the derivation presented in Sect. 2.4.2 to encompass the presence of observation noise.

2.4.3.1 Separate Decoding and Fusion

In the case of separate decoding and fusion, only the expression of the probability $p_{\text{ch}}^{\text{ideal}}$ in (2.44) and (2.45) need to be modified. In particular, by using the total probability theorem [9], one can write

$$\begin{aligned} p_{\text{ch}}^{\text{noisy}} &= \mathbb{P}\{c_{i,\text{rx}} = 1 | H_\ell\} \quad i = 1, \ldots, n, \ \ell = 0, 1 \\ &= p_{\text{ch}}^{\text{ideal}}[1 - Q(\tau - s \cdot \ell)] + (1 - p_{\text{ch}}^{\text{ideal}}) Q(\tau - s \cdot \ell) \end{aligned}$$

where the sensors' decisions $\{c_i^{(\ell)}\}$ are done as outlined in Sect. 2.1.1 and $p_{\text{ch}}^{\text{ideal}}$ is the final BER, which depends on the presence/absence of distributed channel coding, as shown in Sect. 2.4.2.

In a scenario with M observations at each sensor, expression (2.46) for $p_{\text{ch}}^{\text{ideal}}$ has to be similarly modified. In particular, one obtains:

$$p_{\text{ch}}^{\text{noisy}} = \sum_{i=k_{\text{NC}}}^{M} \binom{M}{i} [g(p, \ell)]^i [1 - g(p, \ell)]^{M-i} \tag{2.54}$$

where $g(p, \ell) \triangleq p[1 - Q(\tau - s \cdot \ell)] + (1 - p) Q(\tau - s \cdot \ell)$.

2.4.3.2 Joint Decoding and Fusion

In the case of hard-output detection followed by joint decoding/fusion, expression (2.48) for the phenomenon estimate in a scenario with multiple observations at the sensors has to be modified, similarly to (2.54), as follows:

$$\begin{aligned} P_{\text{e,noisy}}^{\text{mult.obs.}} = &\frac{1}{2} \sum_{i=k_{\text{M}}}^{n \times M} \binom{n \times M}{i} [g(p, 1)]^i [1 - g(p, 1)]^{n \times M - i} \\ &+ \frac{1}{2} \sum_{i=0}^{k_{\text{M}}-1} \binom{n \times M}{i} [1 - g(p, 0)]^i [g(p, 0)]^{n \times M - i}. \end{aligned} \tag{2.55}$$

We now derive the MAP decoding/fusion strategy for the coded scenarios in the presence of noisy observations at the sensors. In the case of hard-output detection followed by (hard-input) joint decoding/fusion, in order to take into account the observation noise statistics expression (2.48) has to be modified as follows:

$$\widehat{H} = \underset{j=0,1}{\text{argmax}} \, \mathbb{P}\{H_j | \boldsymbol{c}_{\text{rx}}\} = \underset{j=0,1}{\text{argmax}} \prod_{i=1}^{n_{\text{cod}}} \mathbb{P}\{c_{i,\text{rx}} | H_j\}$$

where the irrelevant term $P(H_j) = p_j = 1/2$ has been discarded and the probability $P\big(c_{i,\mathrm{rx}}|H_j\big)$ can be written, after a few manipulations, as

$$\mathbb{P}\{c_{i,\mathrm{rx}}|H_j\} = \begin{cases} (1-p)[1-Q(\tau - s\cdot j)] + pQ(\tau - s\cdot j) & \text{if } c_{i,\mathrm{rx}} = 0 \\ p[1-Q(\tau - s\cdot j)] + (1-p)Q(\tau - s\cdot j) & \text{if } c_{i,\mathrm{rx}} = 1. \end{cases}$$

In a coded scenario with joint detection/decoding/fusion, the MAP estimation strategy (2.51) has to be modified as follows:

$$\widehat{H} = \underset{j=0,1}{\operatorname{argmax}} \prod_{i=1}^{n_{\mathrm{cod}}} \mathbb{P}\{r_i|H_j, f_i\}$$

which can be rewritten, after a few manipulations, as

$$\frac{\prod_{i=1}^{n_{\mathrm{cod}}} \Upsilon(0, r_i, f_i)}{\prod_{i=1}^{n_{\mathrm{cod}}} \Upsilon(1, r_i, f_i)} \underset{H_1}{\overset{H_0}{\gtrless}} 1$$

where

$$\Upsilon(m, r_i, f_i) \triangleq \Phi(\tau - m\cdot s)\exp\left(-2\frac{r_i f_i\sqrt{E_{\mathrm{c}}}}{N_0}\right) + [1-\Phi(\tau - m\cdot s)]\exp\left(2\frac{r_i f_i\sqrt{E_{\mathrm{c}}}}{N_0}\right).$$

2.4.4 Impact of Noisy Communication Links Towards the Relay

The previous derivations in coded scenarios are based on the assumption of ideal communication links between the sensors and the relay. In this subsection, we briefly discuss on the impact of *noisy* communication links between the sensors and the relay. Neither analytical derivation nor numerical results will be presented. The considerations which will be carried out are simply meant to give some guidelines on the benefits brought by the distributed use of properly designed block error correction codes.

We first consider the case with *ideal* observations at the sensors. In Fig. 2.29, we give a pictorial description of how the communication noise influences data transmission to the relay. As previously seen, two possible codewords are selected at the sensors and relay, namely $\boldsymbol{c}^{(0)}$ and $\boldsymbol{c}^{(1)}$, which are shown, in Fig. 2.29, as a filled circle and an empty circle, respectively.

- In the scenario with no communication noise between the sensors and the relay (case (a)), we denote the Hamming distance between the two codewords as d. If $\boldsymbol{c}^{(0)} = \mathbf{0}$ and $\boldsymbol{c}^{(1)} = \mathbf{1}$, then $d = n_{\mathrm{cod}}$. The presence of noisy communication links from the sensors and the relay to the AP is such that the word $\boldsymbol{c}_{\mathrm{rx}}$ (one of the $2^{n_{\mathrm{cod}}}$ possible binary sequences of length n_{cod}) received at the AP may be different from the codeword transmitted by the sensors and the relay. In particular, $\boldsymbol{c}_{\mathrm{rx}}$

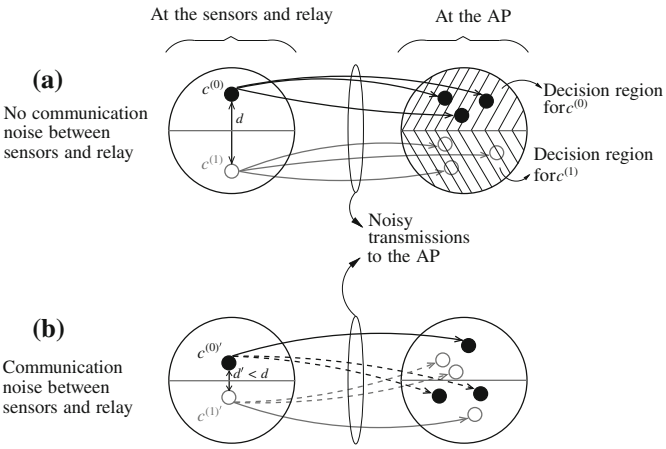

Fig. 2.29 Codebook perspective on the considered distributed detection schemes: **a** ideal communication links between sensors and relay and **b** noisy communication links. In each case, on the left the two possible codewords at sensors and relay are shown, whereas on the right possible received words at the AP are shown

may not even be a codeword. Decoding and fusion at the AP corresponds to associating the received word to one of the information sequences **0** or **1**. It is intuitive that the larger is d, the more robust is the system against communication noise in the links to the AP.

- In the presence of communication noise between the sensors and the relay (case b), the latter may receive a sequence of bits which differs from that sent by the sensors. Therefore, the parity bits generated by the relay may lead to the association of H_0 and H_1 to two codewords $\boldsymbol{c}^{(0)'}$ and $\boldsymbol{c}^{(1)'}$ which are at a distance $d' < d$. As a consequence of this decreased distance, the system performance will be worse than in the previous scenario, since the probability of associating (through decoding and fusion) the received word to the wrong phenomenon status will increase. This can be understood from the codebook scenario at the AP, where the received word at the AP might belong to the portion of the signal space which is associated (by decoding and fusion) to the wrong phenomenon status.

The presence of *noisy* observations may lead to the association of the phenomenon statuses H_0 and H_1 to two codewords $\boldsymbol{c}^{(0)''}$ and $\boldsymbol{c}^{(1)''}$ at a distance smaller than d. In particular, in the presence of both (i) observation noise and (ii) communication noise from the sensors to the relay, when the intensities of these two noises are sufficiently small, their negative effects tend to add, so that the distance d'' between $\boldsymbol{c}^{(0)''}$ and $\boldsymbol{c}^{(1)''}$ might be even smaller than d'.

Obviously, an open problem is to quantify precisely the decrease of the error correction capability t of the code in the presence of noisy communication links between the sensors and the relay. In fact, the parameter t depends on the particular structure (codebook) of the considered error correction code. An interesting

research direction is the design of robust (fault tolerant) error correcting codes for the proposed distributed detection schemes.

2.4.5 Numerical Results

We resort to Monte Carlo simulations to evaluate the probability of decision error with the devised MAP detection/decoding/fusion strategies presented in Sects. 2.4.2 and 2.4.3.

In order to make the detection/decoding process at the input of the AP more effective, *soft-input* decoding/fusion (either separate or joint), rather than hard-input decoding/fusion, can be considered. In Fig. 2.30, the probability of decision error is shown, as a function of the SNR at the AP, in a scenario with $n = 16$ sensors, AWGN communication links (similar results can be obtained in scenarios with Rayleigh faded communication links), and *error-free* observations at the sensors. Six coding strategies are considered: (i) uncoded, (ii) (31,16) BCH [36, p. 438] (the corresponding BCH code has $t = 3$)[12] coded with hard-input and separate decoding/fusion, (iii) (31,16) BCH coded with soft-input and joint decoding/fusion, (iv) with $M = 2$ observations and joint decoding/fusion, (v) with $M = 3$ observations and separate decoding/fusion, and (vi) with $M = 3$ observations and joint decoding/fusion. One can observe that the probability of decision error in coded scenarios shows a "waterfall" behavior, which is due to the concatenation of the decoding and fusion operations. However, the improvement brought by the presence of distributed channel coding, with respect to schemes with multiple observations, becomes apparent at very low probabilities of decision error, which may not be of practical interest. One can observe that the coded network with soft-input and joint decoding/fusion at the AP has a performance significantly better than that associated with the schemes with hard-input and separate decoding/fusion. This is to be expected, since in a scenario with soft-input decoding no information is lost upon reception of the observables from the communication links. Note, however, that in this case as well the proposed coded scheme outperforms a scheme with multiple observations only at very low values of the probability of decision error.

In Fig. 2.31, the probability of decision error is shown, as a function of the BER p at the output of the AP detector, in a scenario with $n = 16$ sensors and *noisy* phenomenon observations. Two values for the observation SNR are considered: (a) 20 dB and (b) 10 dB. The performance is evaluated with six sensor network architectures: (i) uncoded, (ii) (31,16) BCH coded with separate decoding/fusion, (iii) (31,16) BCH coded with joint decoding/fusion, (iv) with $M = 2$ observations and joint decoding/fusion, (v) with $M = 3$ observations and separate

[12] We remark that the BCH is one of the block channel codes that it is possible to consider. However, the same results would be asymptotically obtained with any code with $t = 3$.

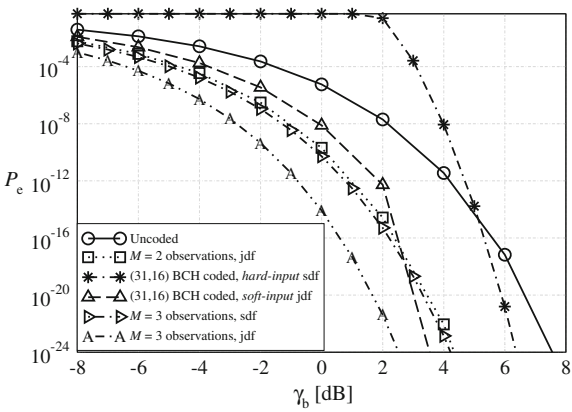

Fig. 2.30 Probability of decision error, as a function of the SNR at the AP, in a scenario with $n = 16$ sensors, AWGN communication links, and *error-free* phenomenon observations. Various coding strategies are considered

decoding/fusion, and (vi) with $M = 3$ observations and joint decoding/fusion. In the case of high observation SNR (e.g., in Fig. 2.31a), the phenomenon observations at the sensors are practically error-free and, therefore, the network performance is similar to that in Fig. 2.30. When the observation SNR decreases (e.g., in Fig. 2.31b), instead, the proposed detection/decoding/fusion strategies are not effective, since the quality of the sensors' observations heavily affects the system performance, and this is more pronounced in the presence of joint decoding/fusion. One can observe that the probability of decision error curve reaches a floor, due to the observation noise (which is independent of the communication noise). As before, the schemes with multiple observations at the sensors outperform those with block channel coding.

Finally, we investigate the performance of the proposed distributed schemes in *large scale* sensor networks, by using an Low-Density Parity-Check (LDPC) code and the sum–product (SP) decoding algorithm. In particular, we consider a (3,6) regular and systematic LDPC code: the systematic bits of the codeword correspond to the n decisions sent by the sensors, whereas the $n_{\text{cod}} - n$ parity bits are generated by the relay node. The LDPC code is constructed in a *random* fashion, according to an algorithm, which exploits an idea similar to the progressive edge growth (PEG) algorithm presented in [37]. In Fig. 2.32, the probability of decision error is shown, as a function of the SNR at the AP, in a scenario with $n = 100$ sensors, AWGN communication links, and *noisy* phenomenon observations. Three sensor network architectures are considered: (i) LDPC coded with standard SP decoding [38, 39], (ii) LDPC coded with *enhanced* (as described in the following) channel Logarithmic Likelihood Ratios (LLRs), and (iii) with $M = 2$ observations and separate decoding/fusion. Two values for the observation SNR are considered: (i) 10 dB (dashed lines) and (ii) 20 dB (solid lines). While in the LDPC coded case with standard SP decoding the channel LLRs (input at the variable nodes of the LDPC bipartite graph) do not take into account the observation noise, in the enhanced SP decoding case the channel LLRs are modified by properly taking into

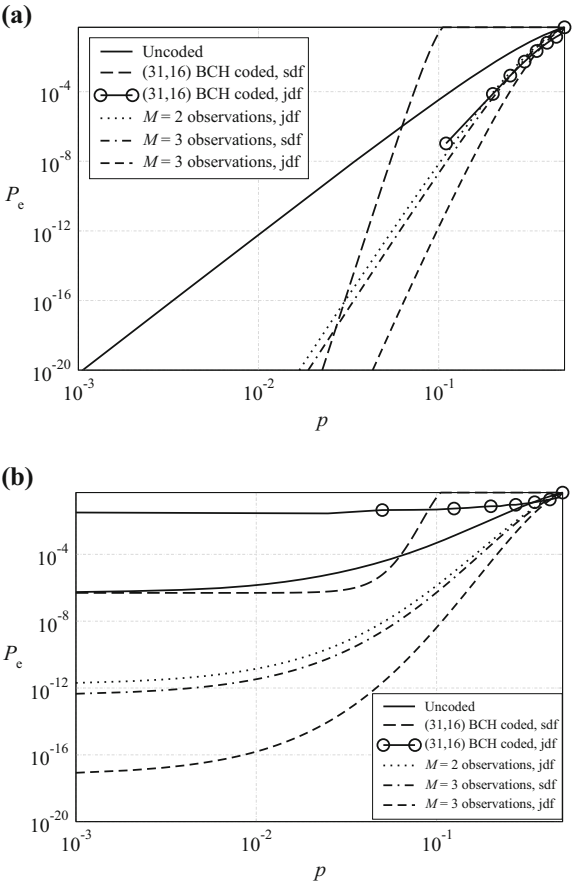

Fig. 2.31 Probability of decision error, as a function of the BER p at the output of the detector, in a scenario with $n = 16$ sensors and *noisy* phenomenon observations. Two values for the observation SNR are considered: **a** 20 dB and **b** 10 dB. Various sensor network architectures are considered

account the observation noise. The modified channel LLRs can be expressed as follows:

$$\mathcal{L}^{(i)}_{\text{ch}-\text{enhanced}} = \mathcal{L}_{\text{ch}} + \mathcal{L}^{(i)}_{\text{a}-\text{priori}} \quad i = 1, \ldots, n_{\text{cod}}$$

where

$$\mathcal{L}_{\text{ch}} \triangleq \ln \frac{p(r_i|c_i = 0)}{p(r_i|c_i = 1)} = \frac{r_i}{N_0}$$

and

$$\mathcal{L}^{(i)}_{\text{a}-\text{priori}} \triangleq \ln \frac{\mathbb{P}\{c_i = 0\}}{\mathbb{P}\{c_i = 1\}} = \begin{cases} \ln \frac{\Upsilon(0,-r_i,1)}{\Upsilon(1,-r_i,1)} & \text{if } i = 1, \ldots, n \\ 0 & \text{if } i = n+1, \ldots, n_{\text{cod}} \end{cases}$$

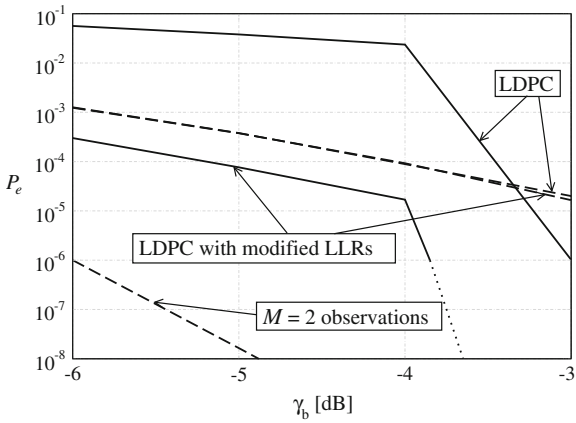

Fig. 2.32 Probability of decision error, as a function of the SNR at the AP, in a scenario with $n = 100$ sensors, AWGN communication links, and *noisy* phenomenon observations. Two values for the observation SNR are considered: (i) 10 dB (*dashed lines*) and (ii) 20 dB (*solid lines*). Various sensor network architectures are considered

where Υ has been defined in Sect. 2.4.3.2. From the results in Fig. 2.32, one can observe that the use of multiple observations is still the winning strategy also in a large-scale sensor network.[13] However, the enhanced LPDC coded scheme (with modified channel LLRs) outperforms the LDPC coded scheme at large observation SNRs, since a statistical knowledge of the observation noise helps the decoding process. In fact, when the communication noise level is too high, a communication error might compensate an error in the phenomenon estimation at the sensors (due to a too high observation noise level). On the other hand, when the communication links to the AP are reliable (i.e., the communication noise is sufficiently small) an error in the phenomenon estimation might not be compensated and, therefore, the AP might not be able to correctly reconstruct the phenomenon status. Finally, note that in the standard LDPC coded case the performance with an observation SNR equal to 10 dB is better than that associated with an observation SNR equal to 20 dB when the SNR at the AP is sufficiently low. This is due to the fact that for small values of the observation SNR a larger number of codewords is actually used by the sensor network and, consequently, the error correction capabilities of the LDPC code are better exploited. However, when the SNR at the AP increases, the "beneficial" impact of the observation noise is reduced by the presence of reliable communication links.

2.5 Concluding Remarks

In this chapter, we have characterized the performance of sensor networks where a spatially constant phenomenon is under observation. First, we have characterized

[13] Note that in Fig. 2.32 only the curve with observation SNR equal to 10 dB is shown in the case with multiple observations. The curve associated with an observation SNR equal to 20 dB and multiple observations is even lower.

the behavior of clustered sensor networks with distributed detection in the presence of multi-level majority-like information fusion. Upon the derivation of a communication-theoretic analytical framework, we have shown that, in the considered scenarios, uniform clustering, i.e., balanced tree network architectures, leads to a lower probability of decision error than non-uniform clustering, i.e., unbalanced tree network architectures. In the former case, the probability of decision error depends *only* on the number of decision levels and *not* on the specific clustering configuration. An information-theoretic perspective has also been presented. Then, the impact of noisy communication links has been investigated. Our results show that the presence of noise in the communication links has a strong bearing on the ultimate achievable performance.

Then, an analytical framework to compute the *network lifetime* of clustered sensor networks subject to a physical layer-oriented QoS condition has been derived. In the presence of ideal reclustering, the network lifetime is the longest possible. On the other hand, in the presence of a fixed clustered configuration, our results show that the number of clusters has a strong impact on the network lifetime. More precisely, the network lifetime is maximized if there are a *few large clusters* (at most four). In all cases, the QoS condition has a strong impact on the network lifetime: the more stringent this condition is, the shorter the network lifetime is. We have also evaluated the cost associated with the reclustering procedure, from both *time delay* and *energy consumption* perspectives. Our results show that reclustering is not useful when phenomenon observations are *rare*, since the network spends more time in transferring control messages than useful data. The impact of noisy communication links, modeled as BSCs, on the network lifetime has also been investigated, showing that the higher the noise level, the shorter the network lifetime. However, also in this scenario reclustering can prolong the network lifetime.

Although the previous analysis was based on the assumption of constant sensor SNR across the sensors, we have proposed an analytical framework to take into account different observation SNRs not known at the AP. In order to model this scenario, four possible sensor SNR profiles (linear, quadratic, cubic, and hyperbolic) have been introduced and we have characterized them by using a *slope coefficient* and the *maximum sensor SNR*. For increasing steepness of the (ordered) sensor SNR profile, i.e., for an increasingly irregular realistic sensor SNR profile, the best performance is obtained by selecting a lower number of sensors (those with highest SNRs). In a scenario with common *average* sensor SNR, the profile which guarantees the best performance is the *cubic*. This is due to the fact that it corresponds to the profile with the largest (in relative terms) number of sensors with SNR higher than the average value. Therefore, a general conclusion is that, for a given *average sensor SNR*, the best performance is obtained when the variance of the sensor SNR is large, i.e., the sensor SNR profile is irregular. The presence of noisy communication links has also been considered. In this case, we have shown that the more irregular the sensor SNR profile, the milder the impact of the noise level in the communication links.

The analytical framework has been enriched with simulation and experimental results (in terms of probability of decision error, throughput, and delay) relative to IEEE 802.15.4-based clustered sensor networks with information fusion. The obtained results confirm the validity of our analytical framework in realistic networking scenarios. Moreover, it has been possible to characterize realistic SNR profiles.

Finally, we have studied how to combine detection, decoding, and fusion at the AP in sensor networks for distributed detection of a spatially constant binary phenomenon. To this end, we have embedded simple distributed channel codes (either block or repetition) into sensor network architectures. The performance of the proposed schemes has been analyzed in scenarios with noisy observations and communications. In all cases, the use of *multiple observations* (i.e., repetition coding) guarantees the best performance, with respect to simple systematic block coding strategies, for practical values of the probability of decision error. This leaves the design of powerful distributed channel codes as an open problem. Considering scenarios with distributed LDPC coding, our results show that knowledge, at the AP, of the observation noise can significantly improve the decoding process, i.e., it can help in reducing the negative effects of the communication noise.

2.6 Further Readings

Recent years have witnessed an increasing interest for the use of distributed detection techniques in sensor networks [40], especially for civilian applications [41], e.g., environmental monitoring [42]. The application of distributed detection techniques in the military field has, on the other hand, a long history. In all cases, the goal of a sensor network with distributed detection is to identify the status of a phenomenon of interest through a collaborative action of the sensors [43]. The increasing interest for sensor networks has, therefore, spurred a significant activity on the design of efficient distributed detection techniques, in order to obtain fault-tolerant networks with the longest possible lifetime [44].

Several communication-theoretic-oriented approaches have been proposed to study decentralized detection [45–52]. In [1], the authors follow a Bayesian approach for the minimization of the probability of decision error at the AP and study optimal fusion rules. Most of the proposed approaches are based on the assumption of *ideal* communication links between the sensors and the AP. However, in a realistic communication scenario, these links are likely to be *noisy* [53]. The impact of noisy communication links on the design of optimal fusion rules is evaluated in [3, 54–57]. A practical and widely used model for the noisy communication links is the BSC [3, 49, 54–56]. In [3], a few techniques are proposed to make the system more robust against the noise. In [51], the author considers Minimum Mean Square Error (MMSE) parameter estimation in sensor networks. Use of censoring algorithms at the sensors has also been studied for the

design of decentralized detection schemes [58]. In [59], the authors analyze aspects related to compression of observed data (using distributed source coding) and data transmission.

Information-theoretic approaches have also been proposed for the study of sensor networks with decentralized detection. In [50], the authors propose a framework to characterize a sensor network in terms of its entropy and false alarm/missed detection probabilities. Information theory has also been used to tackle the problem of optimally placing sensors over a given surface to meet the chosen design criterion. In [60], the mutual information is evaluated in a scenario with censoring sensors which transmit their local likelihood ratios, by maximizing the probability of correct decision [61]. In order to optimally place the sensors over a given surface, system entropy and mutual information are considered in [62, 63], respectively. In [64], an information-theoretic approach is proposed to solve, with limited complexity, the problem of sensor selection and placement for target localization and tracking. Decentralized detection algorithms, based on the evaluation of the sensor network mutual information, have also been proposed to design intelligent systems that recognize, in a robust manner, a target in a scene which rapidly changes [65].

The impact of communication constraints, e.g., limited bandwidth and presence of noise, is considered in [66], where a randomization paradigm for decentralized detection is proposed to overcome the communication bottle-neck. In [7], the authors consider the problem of decentralized detection in *wireless* sensor networks where communication links are affected by fading. In the latter scenario, the optimal distributed detection strategy is first derived, on the basis of the integration of the communication and fusion phases, and then suboptimal (requiring a limited a priori knowledge of the channel state) strategies are developed. This approach is further extended in [54], where the authors optimize the local decision strategy in sensor networks with fading, and in [67], where the authors propose a decentralized detection strategy based on censoring sensors, which transmit only when their local likelihood ratios are sufficiently large.

For what concerns the issue of energy efficiency, motivated by recent theoretical results in the area of network coding [68–73], significant research activity has been devoted to the development of specific channel coding strategies. Although preliminary works focus on scenarios with ideal communication channels, the impact of communication noise has also been investigated [74]. Moreover, distributed network coding strategies for the multi-access relay channel, i.e., a channel where source nodes can send their information to the destination through a common relay node, have been investigated [75, 76].

The problem of extending the sensor network lifetime is a direct consequence of the energy efficiency in scenarios with battery-powered nodes. In particular, the derivation of upper bounds for the sensor network lifetime has been exploited. In [77–85], various analyses are carried out according to the particular sensor network architecture and the definition of sensor network lifetime. In [86], a simple formula, independent of these parameters, is provided for the computation of the sensor network lifetime and a Medium Access Control (MAC)

protocol is proposed to maximize the sensor network lifetime. In [87], a distributed MAC protocol is designed in order to maximize the network lifetime. In [88], network lifetime maximization is considered as the main criterion for the design of sensor networks with data gathering. In [89], the authors consider a realistic sensor network with nodes equipped with TinyOS, an event-based operating system for networked sensor motes. In this scenario, the network lifetime is evaluated as a function of the average distance of the sensors from the central data collector. In [90], an analytical framework, based on the Chen-Stein method of Poisson approximation, is proposed in order to find the critical time at which isolated nodes, i.e., nodes without neighbors in the network, begin to appear, due to the deaths of other nodes. Although this method is derived for generic networks where nodes are randomly deployed and can die in a random manner, this can also be applied to sensor networks. Finally, an important area of application of wireless sensor networking is the medical field. In [91], an analysis of network lifetime using IEEE 802.15.4 sensor networks is derived for this kind of applications.

References

1. W. Shi, T.W. Sun, R.D. Wesel, Quasi-convexity and optimal binary fusion for distributed detection with identical sensors in generalized gaussian noise. IEEE Trans. Inform. Theory **47**(1), 446–450 (2001)
2. G. Ferrari, R. Pagliari, Decentralized detection in sensor networks with noisy communication links. In: F. Davoli, S. Palazzo, S. Zappatore (eds) *Distributed Cooperative Laboratories: Networking, Instrumentation, and Measurements (Signals and Communication Technology)* (Springer, New York, 2006)
3. G. Ferrari, R. Pagliari, Decentralized binary detection with noisy communication links. IEEE Trans. Aerosp. Electron. Syst. **42**(4), 1554–1563 (2006)
4. B. Chen, L. Tong, P.K. Varshney, Channel aware distributed detection in wireless sensor networks. IEEE Signal Process. Mag. **23**(4), 16–26 (2006). Special Issue on Distributed Signal Processing for Sensor Networks
5. Q. Cheng, B. Chen, P.K. Varshney, Detection performance limits for distributed sensor networks in the presence of non-ideal channels. IEEE Trans. Wirel. Commun. **5**(11), 3034–3038 (2006)
6. R. Niu, B. Chen, P.K. Varshney, Fusion of decisions transmitted over Rayleigh fading channels in wireless sensor networks. IEEE Trans. Signal Process. **54**(3), 1018–1027 (2006)
7. B. Chen, R. Jiang, T. Kasetkasem, P.K. Varshney, Channel aware decision fusion in wireless sensor networks. IEEE Trans. Signal Process. **52**(12), 3454–6458 (2004)
8. G. Ferrari, M. Martalò, R. Pagliari, Decentralized detection in clustered sensor networks. IEEE Trans. Aerosp. Electron. Syst., **47**(2), April (2011)
9. A. Papoulis, *Probability, Random Variables and Stochastic Processes* (McGraw-Hill, New York, 1991)
10. R. Meester, R. Roy, *Continuum Percolation* (Cambridge University Press, Cambridge, 1996)
11. G.R. Grimmet, *Percolation* (Springer, New York, 1999)
12. O. Dousse, F. Baccelli, P. Thiran, Impact of interferences on connectivity in ad hoc networks, in *Proceedings of IEEE Conference on Computer Communication (INFOCOM)*, vol. 3, San Francisco, USA, April 2003, pp. 1724–1733

13. L. Booth, J. Brook, M. Franceschetti, R. Meester, Continuum percolation and the geometry of wireless networks. Ann. Appl. Prob. **13**(2), 722–733 (2003)
14. O.K. Tonguz, G. Ferrari, *Ad Hoc Wireless Networks: A Communication-Theoretic Perspective* (Wiley, Chichester, 2006)
15. T.M. Cover, J.A. Thomas, *Elements of Information Theory* (Wiley, New York, 1991)
16. G. Ferrari, M. Martalò, R. Pagliari, On multi-level decentralized detection in sensor networks, in *Proceedings of International Conference on Intelligent Systems and Computing: Theory and Applications (ISYC)*, Ayia Napa, Cyprus, July 2006
17. Opnet Website, http://www.opnet.com
18. N. I. of Standards and T. N. Website, http://www.nist.gov
19. G. Ferrari, P. Medagliani, M. Martalò, A. Muzzini, Zigbee wireless sensor networks with data fusion, in *Proceedings of International Symposium on Communications, Control and Signal Processing (ISCCSP)*, St. Julians, Malta, March 2008, pp. 472–477
20. Cross-Bow, Wireless sensor networks, http://www.xbow.org
21. Atmel Corporation, Atmel microcontroller, http://www.atmel.com/atmel/acrobat/doc2467.pdf
22. Texas Instruments, RF/IF and ZigBee solutions, http://www.ti.com/
23. R.E. Ziemer, *Elements of Engineering Probability & Statistics* (Prentice-Hall, Upper Saddle River, 1997)
24. G. Ferrari, M. Martalò, Extending the lifetime of sensor networks through adaptive reclustering, EURASIP J. Wirel. Commun. Netw. **2007**, 20 pages, Special Issue on "Novel Techniques for Analysis & Design of Cross-Layer Optimized Wireless Sensor Networks", article ID 31809. doi:10.1155/2007/31809
25. J.H. Conway, R.K. Guy, *The Book of Numbers* (Springer, New York, 1996)
26. IEEE 802.15.4 Std, *Wireless Medium Access Control (MAC) and Physical Layer (PHY) Specifications for Low-Rate Wireless Personal Area Networks (LR-WPANs)* (IEEE Computer Society Press, 2003), pp. 1–679, ISBN: 0-7381-3677-5
27. G. Ferrari, P. Medagliani, S. Di Piazza, M. Martalò, Wireless sensor networks: performance analysis in indoor scenarios. EURASIP J. Wirel. Commun. Netw. **2007**, 14 pages (2007), Special Issue on "MobileMAN (Mobile Multi-hop Ad Hoc Networks): From Theory to Reality, article ID 81864. doi:10.1155/2007/81864
28. J. Ma, M. Gao, Q. Zhang, L.M. Ni, W. Zhu, Localized low-power topology control algorithms in IEEE 802.15.4-based sensor networks, in *Proceedings of IEEE International Conference on Distributed Computing Systems*, Columbus, OH, USA, June 2005, pp. 27–36
29. G. Ferrari, P. Medagliani, M. Martalò, Performance analysis of Zigbee wireless sensor networks with relaying, in *Proceedings of International Workshop on Distributed Cooperative Laboratories (Ingrid)*, Santa Margherita Ligure, Italy, April 2007
30. G. Ferrari, R. Pagliari, M. Martalò, Decentralized binary detection with non-constant SNR profile at the sensors. Int. J. Sens. Netw. **4**(1), 23–36 (2008). Special Issue on Energy-Efficient Algorithm and Protocol Design in Sensor Networks
31. J. Tsitsiklis, Decentralized detection by a large number of sensor. Math. Control Signals Syst. (MCSS) **1**(2), 167–182 (1988)
32. S. Alhakeem, P.K. Varshney, A unified approach to the design of decentralized detection systems. IEEE Trans. Aerosp. Electron. Syst. **31**(1), 9–20 (1995)
33. P. Willett, B. Tober, P. Swaszek, Fully-connected non-hierarchical decentralized detection networks, in *Proceedings of IEEE Conference on Control Applications*, Dayton, OH, USA, September 1992, pp. 404–409
34. A.B. Carlson, P.B. Crilly, J.C. Rutledge, *Communication Systems, An Introduction to Signals and Noise in Electrical Communication*, 4th edn (McGraw-Hill, New York, 2002)
35. A.F. Molisch, *Wireless Communications* (Wiley, Chichester, 2005)
36. J.G. Proakis, *Digital Communications*, 4th edn (McGraw-Hill, New York, 2001)
37. X. Hu, E. Eleftheriou, D. Arnold, Regular and irregular progressive edge-growth tanner graphs. IEEE Trans. Inform. Theory **51**(1), 386–398 (2005)
38. R.G. Gallager, *Low Density Parity Check Codes* (MIT Press, Cambridge, 1963)

39. F.R. Kschischang, B.J. Frey, H.A. Loeliger, Factor graphs and the sum-product algorithm. IEEE Trans. Inform. Theory **47**(2), 498–519 (2001)
40. I. Akyildiz, W. Su, Y. Sankarasubramaniam, E. Cayirci, A survey on sensor networks. IEEE Commun. Mag. **40**(8), 102–114 (2002)
41. C.Y. Chong, S.P. Kumar, Sensor networks: evolution, challenges, and opportunities. Proc. IEEE **91**(8), 1247–1256 (2003)
42. S.N. Simic, S. Sastry, Distributed environmental monitoring using random sensor networks, in *Proceedings of International Work. on Inform. Processing in Sensor Networks (IPSN)*, Palo Alto, CA, USA, April 2003, pp. 582–592
43. J.N. Tsitsiklis, Decentralized detection. In: H.V. Poor, J.B. Thomas (eds) *Advances in Statistical Signal Process*, vol. 2 (JAI Press, Greenwich, 1993), pp. 297–344
44. R. Verdone, D. Dardari, G. Mazzini, A. Conti, *Wireless Sensor and Actuator Networks: Technologies, Analysis and Design* (Elsevier, London, 2008)
45. R.R. Tenney, N.R. Sandell, Detection with distributed sensors. IEEE Trans. Aerosp. Electron. Syst. **17**(4), 501–510 (1981)
46. A. Reibman, L. Nolte, Design and performance comparison of distributed detection networks. IEEE Trans. Aerosp. Electron. Syst. **23**(6), 789–737 (1987)
47. R. Viswanathan, P.K. Varshney, Distributed detection with multiple sensors—Part I: fundamentals. Proc. IEEE **85**(1), 54–63 (1997)
48. J.F. Chamberland, V.V. Veeravalli, Decentralized detection in sensor networks. IEEE Trans. Signal Process. **51**(2), 407–416 (2003)
49. H. Gharavi, K. Ban, Multihop sensor network design for wide-band communications. Proc. IEEE **91**(8), 1221–1234 (2003)
50. I.Y. Hoballah, P.K. Varshney, An information theoretic approach to the distributed detection problem. IEEE Trans. Inform. Theory **35**(5), 988–994 (1989)
51. Z.Q. Luo, An isotropic universal decentralized estimation scheme for a bandwidth constrained ad hoc sensor network. IEEE J. Select. Areas Commun. **23**(4), 735–744 (2005)
52. R. Blum, A. Kassam, H. Poor, Distributed detection with multiple sensors: Part II. Proc. IEEE **85**(1), 64–79 (1997)
53. T.S. Rappaport, *Wireless Communications, Principles & Pratice*, 2nd edn (Prentice-Hall, Uper Saddle River, 2002)
54. B. Chen, P.K. Willett, On the optimality of the likelihood-ratio test for local sensor decision rules in the presence of nonideal channels. IEEE Trans. Inform. Theory **51**(2), 693–699 (2005)
55. M. Madishetty, V. Kanchumarthy, C.H. Gowda, R. Viswanathan, Distributed detection with channel errors, in *Proceedings of Southeastern Symposium on System Theory (SSST)*, Tuskegee University, AL, USA, March 2005, pp. 302–306
56. A.R. Reibman, L.W. Nolte, Optimal design and performance of distributed signal detection systems with faults. IEEE Trans. Acoust., Speech Signal Process. **38**(10), 1771–1782 (1990)
57. S.C.A. Thomopoulos, L. Zhang, Distributed decision fusion in the presence of networking delays and channel errors. Inform. Sci. **66**(1–2), 91–118 (1992)
58. N. Patwari, A.O. Hero, Hierarchical censoring for distributed detection in wireless sensor networks, in *Proceedings of International Conference on Acoustics, Speech and Signal Processing (ICASSP)*, vol 4. Hong Kong, April 2003, pp. 848–851
59. M. Gastpar, M. Vetterli, P.L. Dragotti, Sensing reality and communicating bits: a dangerous liaison. IEEE Signal Process. Mag. **23**(4), 70–83 (2006)
60. K. Yamasaki, T. Ohtsuki, Design of energy-efficient wireless sensor networks with censoring, on–off, and censoring and on–off sensors based on mutual information, in *Proceedings of IEEE Vehicular Technology Conference (VTC)*, vol 2, Stockholm, Sweden, May 2005, pp. 1312–1316
61. Y. Lin, B. Chen, P.K. Varshney, Decision fusion rules in multi-hop wireless sensor networks. IEEE Trans. Aerosp. Electron. Syst. **41**(2), 475–488 (2005)
62. N.A.C. Cressie, *Statistics for Spatial Data* (Wiley, New York, 1993)

63. C. Guestrin, A. Krause, A.P. Singh, Near-optimal sensor placement in Gaussian processes, in *Proceedings of International Conference on Machine Learning*, vol. 119, Bonn, Germany, August 2005, pp. 265–272
64. H. Wang, K. Yao, D. Estrin, Information-theoretic approaches for sensor selection and placement in sensor networks for target localization and tracking. J. Commun. Netw. **7**(4), 438–449 (2005)
65. T. Ikeda, H. Ishiguro, M. Asada, Adaptive fusion of sensor signals based on mutual information maximization, in *Proceedings of International Conference on Robotics and Automation (ICRA)*, vol 3, Taipei, Taiwan, September 2003, pp. 4398–4402
66. F. Gini, F. Lombardini, L. Verrazzani, Decentralised detection strategies under communication constraints. IEE Proc. Radar Sonar Navig. **145**(4), 199–208 (1998)
67. R. Jiang, B. Chen, Fusion of censored decisions in wireless sensor networks. IEEE Trans. Wirel. Commun. **4**(6), 2668–2673 (2005)
68. R. Ahlswede, N. Cai, S.Y.R. Li, R.W. Yeung, Network information flow. IEEE Trans. Inform. Theory **46**(4), 1204–1216 (2000)
69. S.Y.R. Li, R.W. Yeung, N. Cai, Linear network coding. IEEE Trans. Inform. Theory **49**(2), 371–381 (2003)
70. R. Koetter, M. Medard, An algebraic approach to network coding. IEEE/ACM Trans. Netw. **11**(5), 782–795 (2003)
71. X. Bao, J. Li, Matching code-on-graph with network-on-graph: adaptive network coding for wireless relay networks, in *Proceedings of Allerton Conference on Communication, Control and Computing (ALLERTON)*, Urbana Champaign, IL, USA, September 2005
72. C. Fragouli, E. Soljanin, Information flow decomposition for network coding. IEEE Trans. Inform. Theory **52**(3), 829–848 (2006)
73. D. Tuninetti, C. Fragouli, On the throughput improvement due to limited complexity processing at relay nodes, in *Proceedings of IEEE Symposium on Information Theory (ISIT)*, Adelaide, Australia, September 2005, pp. 1081–1085
74. M. Xiao, T. Aulin, A physical layer aspect of network coding with statistically independent noisy channels, in *Proceedings of IEEE International Conference on Communication (ICC)*, vol 9, Instanbul, Turkey, June 2006, pp. 3996–4001
75. C. Hausl, P. Dupraz, Joint network-channel coding for the multiple-access relay channel, in *Proceedings of IEEE Conference on Sensor and Ad Hoc Communications and Networks (SECON)*, vol 3, New York, NY, USA, June 2006, pp. 817–822
76. C.-C. Chang, H.-N. Lee, Space-time mesh codes for the multiple-access relay network: space vs. time diversity benefits, in *Proceedings of Workshop on Network Coding, Theory, and Applications (NetCod)*, San Diego, CA, USA, January 2007
77. A. Kansal, A. Ramamoorthy, M. Srivastava, G. Pottie, On sensor network lifetime and data distortion, in *Proceedings of IEEE Symposium on Information Theory (ISIT)*, Adelaide, Australia, September 2005, pp. 6–10
78. S. Arnon, Deriving an upper bound on the average operation time of a wireless sensor network. IEEE Commun. Lett. **9**(2), 154–156 (2005)
79. F. Ordonez, B. Krishnamachari, Optimal information extraction in energy-limited wireless sensor networks. IEEE J. Select. Areas Commun. **22**(6), 1121–1129 (2004)
80. H. Zhang, J. Hou, On deriving the upper bound of lifetime for large sensor networks, in *Proceedings of ACM International Symposium on Mobile Ad Hoc Networking and Computing (MOBIHOC)*, Tokyo, Japan, May 2004, pp. 121–132
81. Z. Hu, B. Li, On the fundamental capacity and lifetime limits of energy-constrained wireless sensor networks, in *Proceedings of IEEE Real-Time and Embedded Technology and Applications Symp. (RTAS)*, Toronto, Canada, May 2004, pp. 2–9
82. D.M. Blough, P. Santi, Investigating upper bounds on network lifetime extension for cell-based energy conservation techniques in stationary ad-hoc networks, in *Proceedings of ACM International Conference on Mobile Computing and Networking (MOBICOM)*, Atlanta, GA, USA, September 2002, pp. 183–192

83. M. Bhardwaj, T. Garnett, A.P. Chandrakasan, Upper bounds on the lifetime of sensor networks, in *Proceedings of IEEE International Conference on Communication (ICC)*, vol 119, Helsinki, Finland, June 2001, pp. 785–790
84. M. Bhardwaj, A.P. Chandrakasan, Bounding the lifetime of sensor networks via optimal role assignments, in *Proceedings of IEEE Conference on Computer Communications (INFOCOM)*, vol 3, New York, NY, USA, June 2002, pp. 1587–1596
85. V. Rai, R.N. Mahapatra, Lifetime modeling of a sensor network, in *Proceedings of Design, Automation and Test in Europe (DATE)*, vol 1, Messe Munich, Germany, March 2005, pp. 202–203
86. Y. Chen, Q. Zhao, On the lifetime of wireless sensor networks. IEEE Commun. Lett. **9**(11), 976–978 (2005)
87. Q. Zhao, A. Swami, L. Tong, The interplay between signal processing and networking in sensor networks. IEEE Signal Process. Mag. **23**(4), 84–93 (2006)
88. K. Kalpakis, K. Dasgupta, P. Namjoshi, Maximum lifetime data gathering and aggregation in wireless sensor networks, University of Maryland, Baltimore, Tech. Rep., 2002, http://www.csee.umbc.edu/∼kalpakis/
89. M.E.S. Coleri, T.J. Koo, Lifetime analysis of a sensor network with hybrid automata modelling, in *Proceedings of International Workshop on Wireless Sensor Networks and Applications (WSNA)*, Atlanta, USA, September 2002, pp 98–104
90. M. Franceschetti, R. Meester, Critical node lifetime in random networks via the Chen-Stein method. IEEE Trans. Inform. Theory **52**(6), 2831–2837 (2006)
91. N.F. Timmons, W.G. Scanlon, Analysis of the performance of IEEE 802.15.4 for medical sensor body area networking, in *Proceedings of IEEE Conference on Sensor and Ad Hoc Communications and Networks (SECON)*, Santa Clara, CA, USA, October 2004, pp. 16–24

http://www.springer.com/978-3-642-17489-6

Sensor Networks with IEEE 802.15.4 Systems
Distributed Processing, MAC, and Connectivity
Buratti, C.; Martalo', M.; Verdone, R.; Ferrari, G.
2011, XVIII, 250 p., Hardcover
ISBN: 978-3-642-17489-6